

Pair Excitations, Collective Modes and Gauge Invariance in the BCS – Bose-Einstein Crossover Scenario

Ioan Kosztin, Qijin Chen, Ying-Jer Kao, and K. Levin

The James Franck Institute, The University of Chicago, 5640 South Ellis Avenue, Chicago, Illinois 60637

(September 18, 2021)

In this paper we study the BCS Bose Einstein condensation (BEC) crossover scenario within the superconducting state, using a T-matrix approach which yields the ground state proposed by Leggett. Here we extend this ground state analysis to finite temperatures T and interpret the resulting physics. We find two types of bosonic-like excitations of the system: long lived, incoherent pair excitations and collective modes of the superconducting order parameter, which have different dynamics. Using a gauge invariant formalism, this paper addresses their contrasting behavior as a function of T and superconducting coupling constant g . At a more physical level, our paper emphasizes how, at finite T , BCS-BEC approaches introduce an important parameter $\Delta_{pg}^2 = \Delta^2 - \Delta_{sc}^2$ into the description of superconductivity. This parameter is governed by the pair excitations and is associated with particle-hole asymmetry effects which are important for sufficiently large g . In the fermionic regime, Δ_{pg}^2 represents the difference between the square of the excitation gap Δ^2 and that of the superconducting order parameter Δ_{sc}^2 . The parameter Δ_{pg}^2 , which is necessarily zero in the BCS (mean field) limit increases monotonically with the strength of the attractive interaction g . It follows that there is a significant physical distinction between this BCS-BEC crossover approach (in which g is the essential variable which determines Δ_{pg}) and the widely discussed (Coulomb-modulated) phase fluctuation scenario in which the plasma frequency is the tuning parameter. Finally, we emphasize that in the strong coupling limit, there are important differences between the composite bosons which arise in crossover theories, and the usual bosons of the (interacting) Bose liquid. Because of constraints imposed on the fermionic excitation gap and chemical potential, in crossover theories, the fermionic degrees of freedom can never be fully removed from consideration.

PACS numbers: 74.20.-z, 74.20.Fg, 74.25.Nf

I. INTRODUCTION

The observation of an excitation gap above T_c (called the “pseudogap”) in the underdoped cuprate superconductors has been the focus of much current research. Presumably an understanding of this state will help unravel the formal machinery, if not the attractive pairing mechanism behind high temperature superconductivity. It is now widely believed that this state is associated with the underlying superconducting phase, in large part because the (d -wave) symmetry of the pseudogap is found^{1,2} to be the same as that of the excitation gap and order parameter in the $T < T_c$ state. Among viable candidates for the origin of the pseudogap state are phase fluctuation scenarios^{3,4}, d -wave nodal excitation mechanisms⁵ and a BCS Bose-Einstein “crossover picture”^{6–14}.

The goal of the present paper is to discuss the last of these, the crossover scenario within the superconducting state. Our work is directed towards the fundamental issues of the crossover problem, with lesser emphasis on the physics of the cuprates. We present a generalized overview based on a finite temperature T matrix formulation. Our aim is to provide a useful understanding and to extend the physics of the well characterized ground state¹⁵. In the process we establish a clear distinction between incoherent, finite center of mass momentum, pair excitations and order parameter fluctuations (i.e., collective modes), and their respective dynamics. We formulate a gauge invariant description of the electrodynamic response with an emphasis on particle-hole asymmetry which is necessarily very important. Although we introduce a generalized T matrix approach, special attention will be paid to one particular version which has been extensively discussed in our previous work^{8,10–12,16}.

In the BCS Bose-Einstein condensation (BEC) crossover approach, it is presumed that there is a smooth evolution, with increasing attractive coupling constant g , from BCS superconductivity, in which strongly overlapping Cooper pairs form and Bose condense at precisely the same temperature T_c , to a quasi-ideal Bose gas state (to be characterized in more detail below) in which tightly bound fermion pairs (composite bosons) form at temperatures much higher than their Bose condensation temperature T_c . In this latter case there is an excitation gap (pseudogap) for *fermionic* excitations well above T_c . These ideas date back to the late sixties when Eagles¹⁷ first drew attention to the possibility of smoothly interpolating between the BCS and Bose-Einstein ground state descriptions of superconductivity. This was followed by a well known paper by Leggett¹⁵ who presented an interpolation scheme for the ground state based on a variational wave-function, in which the chemical potential μ was self consistently varied (with increasing g) from E_F to large negative values. Nozieres and Schmitt-Rink¹⁸, hereafter referred to as NSR, generalized these previous approaches by presenting a crossover theory for computing T_c . Although this leading order theory was not fully self consistent¹⁹, nevertheless, much of the essential physics pertaining to finite T was summarized in Ref. 18.

With the discovery of the short coherence length cuprates, several groups noted the relevance of this body of theoretical work. Indeed, this recognition was made well in advance of a community-wide appreciation of pseudogap phenomena, which phenomena have only served to re-enforce interest in these crossover schemes. Randeria and co-workers²⁰ were among the first to apply the NSR approach to the cuprates. Micnas *et al*²¹ presented detailed studies of the attractive Hubbard model with varying on-site Coulomb interaction U , and Uemura⁹ noted, on the basis of unusual correlations deduced from μ SR experiments, that the cuprates exhibited aspects of bosonic character, as might be expected in a crossover theory. Our own group¹¹ has also addressed cuprate issues in the past year using the formalism of the present paper.

Attempts to go beyond the NSR scheme at finite T are relatively more recent and almost exclusively restricted to two dimensional systems. Numerical simulations^{22,23} on the attractive Hubbard model, along with numerical^{24,25} and analytical¹³ studies of the so-called FLEX scheme²⁴ have provided some insights. This diagrammatic FLEX approach should be contrasted with an alternative (called the “pairing approximation”) which we^{8,10–12,16} have introduced into the literature and which is based on earlier work by Kadanoff and Martin²⁶, and extended by Patton²⁷. In contrast to the FLEX scheme this latter approach precisely yields BCS theory in the small g limit. What is more important in distinguishing our work from that of others, however, is our direct focus^{10,11} on *crossover effects within the superconducting state*. This is the topic of the present paper, as well, and necessarily requires studies of systems in higher than two dimensions, where T_c is non-zero. The ultimately decisive factor in determining whether these crossover theories or any other alternatives are appropriate for the cuprates, may well come from the predicted behavior below T_c . This fact has also been emphasized by Deutscher²⁸.

II. OVERVIEW OF BCS-BEC CROSSOVER THEORIES

A. Physical Picture at $T = 0$: Previous Work

All crossover theories are based on an underlying “generic” Hamiltonian describing the attractive interaction between fermions with opposite spin orientation (for spin singlet pairing)

$$\mathcal{H} = \sum_{\mathbf{k}\sigma} \epsilon_{\mathbf{k}} c_{\mathbf{k}\sigma}^\dagger c_{\mathbf{k}\sigma} + \sum_{\mathbf{k}\mathbf{k}'\mathbf{q}} V_{\mathbf{k},\mathbf{k}'} c_{\mathbf{k}+\mathbf{q}/2\uparrow}^\dagger c_{-\mathbf{k}+\mathbf{q}/2\downarrow}^\dagger c_{-\mathbf{k}'+\mathbf{q}/2\downarrow} c_{\mathbf{k}'+\mathbf{q}/2\uparrow}, \quad (1)$$

where $c_{\mathbf{k}\sigma}^\dagger$ creates a particle in the momentum state \mathbf{k} with spin σ , and $\epsilon_{\mathbf{k}}$ is the energy dispersion measured from the chemical potential μ (we take $\hbar = k_B = 1$). For the jellium case $\epsilon_{\mathbf{k}} = \mathbf{k}^2/2m - \mu$, while for the lattice case we consider an anisotropic tight-binding model with $\epsilon_{\mathbf{k}} = 2t_{\parallel}(2 - \cos k_x - \cos k_y) + 2t_{\perp}(1 - \cos k_z) - \mu$, where t_{\parallel} (t_{\perp}) is the hopping integral for the in-plane (out-of-plane) motion, and we set the lattice constant $a = 1$. Here we assume a separable pairing interaction $V_{\mathbf{k},\mathbf{k}'} = g\varphi_{\mathbf{k}}\varphi_{\mathbf{k}'}$, where $g = -|g|$ is the coupling strength and the momentum dependence of the function $\varphi_{\mathbf{k}}$, reflects the pairing anisotropy, and its form depends on the particular model under consideration. For the jellium case we take¹⁸ $\varphi_{\mathbf{k}} = (1 + k^2/k_0^2)^{-1/2}$, where $1/k_0$ gives the range of the interaction and represents a soft cutoff in momentum space for the pairing interaction. In the lattice case, $\varphi_{\mathbf{k}} = 1$ for s -wave pairing symmetry, and $\varphi_{\mathbf{k}} = \cos k_x - \cos k_y$ for d -wave symmetry. To simplify the notation, until Sec. V, when the effects of $\varphi_{\mathbf{k}}$ become relevant, we choose to write our equations with $\varphi_{\mathbf{k}} = 1$.

It is important to stress the key assumptions of these crossover theories: (i) only two body fermionic interactions are included. (ii) In calculations of *equilibrium* properties (as distinct from studies of the collective mode of the superconducting order parameter), repulsive Coulomb interactions between fermions are absorbed into the effective pairing interaction $V_{\mathbf{k},\mathbf{k}'}$. These Coulomb effects are presumed to be weak enough so that the attractive interactions driving superconductivity dominate, and it is assumed that Coulomb interactions do *not* occur between fermion pairs or composite bosons.

Using this Hamiltonian, Leggett¹⁵ found that the BCS ground state wavefunction

$$|\Psi\rangle = \prod_{\mathbf{k}} \left(u_{\mathbf{k}} + v_{\mathbf{k}} c_{\mathbf{k}\uparrow}^\dagger c_{-\mathbf{k}\downarrow}^\dagger \right) |\text{vac}\rangle \quad (2)$$

is appropriate to *both* the weakly and strongly interacting limits, provided $v_{\mathbf{k}}^2 = \frac{1}{2}(1 - \epsilon_{\mathbf{k}}/E_{\mathbf{k}})$, $u_{\mathbf{k}}^2 = \frac{1}{2}(1 + \epsilon_{\mathbf{k}}/E_{\mathbf{k}})$, where $E_{\mathbf{k}} = \sqrt{\epsilon_{\mathbf{k}}^2 + \Delta^2}$. Moreover, the explicit parameter Δ and the implicit parameter μ follow from the following two self consistent conditions

$$g^{-1} + \sum_{\mathbf{k}} \frac{1}{2E_{\mathbf{k}}} = 0, \quad (3)$$

and

$$n = 2 \sum_{\mathbf{k}} v_{\mathbf{k}}^2, \quad (4)$$

where n is the electron number density.

In the weak coupling limit, the above equations yield the usual BCS state. By contrast, in the strong coupling (i.e., $g \rightarrow \infty$) limit, for the case of jellium, the system corresponds to a Bose condensation of nonoverlapping and *non-interacting* tightly bound pairs of fermions, which resemble to diatomic molecules. This is an “essentially ideal Bose gas”¹⁸. Indeed, it can be shown¹⁵ that in the strong coupling limit, Eq. (3) can be recast in the form of the Schrödinger equation, written in momentum space, for an *isolated* diatomic molecule, consisting of the two fermions. The strong coupling limit was argued to be slightly more complicated for a lattice of fermions¹⁸ which, at moderate densities, is to be distinguished from jellium. Here a canonical transformation can be used to partially integrate out the fermions and the Pauli principle then leads to hard core repulsions between composite bosons. Nevertheless, even for a lattice, this scheme is viewed as reasonable¹⁸ so that the BCS wave function assumption, or equivalently Eqs. (3) and (4), represent an effective mean field approximation to the solution of the hard core composite boson problem. This essentially ideal Bose gas treatment of the ground state in the strong coupling limit is to be contrasted with the behavior found in the collective mode spectrum, where calculations lead to results similar to those for a weakly interacting Bose gas. These calculations suggest the presence of an *effective* boson-boson interaction in this limit.

Within crossover theories, the $T = 0$ behavior of the Anderson Bogoliubov (AB) mode has been studied in Refs. 29, 30 and 7. In the long wavelength (small \mathbf{q}) limit the dispersion relation of the sound-like AB mode is linear: $\omega = cq$, where c is the AB mode velocity. In weak coupling, the usual BCS limit is obtained for the AB mode velocity $c = v_F/\sqrt{3}$. In strong coupling, c reflects an effective boson-boson interaction³¹ which arises from the Pauli principle. We caution that even though the phrase boson-boson interaction is frequently used here and in the literature, in the composite boson system (within the crossover scenario), these interactions should always be viewed as indirect and associated with the underlying fermionic interactions.

In summary, the $T = 0$ description of the composite boson problem (in the strong coupling limit) represents a cross between ideal and non-ideal Bose-Einstein physics. Whereas, an incomplete condensation at zero temperature is required in order to obtain superfluidity in a “true” Bose system³², in the crossover scenario, the condensation is always complete (at $T = 0$), but, nevertheless the phase mode and superconductivity exist.

B. Physical Picture at Finite $T < T_c$: Present Work

In this section we discuss our general results and physical picture for the finite T crossover problem, at an intuitive level. These results are then re-derived in more detail in Sec. III using a microscopic T-matrix approach. As the temperature is increased above $T = 0$, and the coupling g becomes sufficiently strong, two important effects ensue¹⁰. (i) The excitation gap is no longer the same as (the amplitude of) the superconducting order parameter. (ii) Incoherent pair excitations with non-zero center of mass momentum can be thermally excited. Indeed, points (i) and (ii) are inter-related. The first of these is anticipated as one leaves the BCS regime, where even above T_c , there is expected to be a normal state gap for fermionic excitations; this gap is associated with meta-stable (intermediate g)⁸ or stable (large g) pairs. It is natural to presume, as we have found,¹⁰ that these effects persist below T_c . Indeed, if there is an excitation gap at T_c , in any second order superconducting transition, this gap must necessarily be different from the superconducting order parameter, at least, at and slightly below T_c .

The second of these two points was noted in Ref. 18. These pair excitations are related to the “particle” excitation branch of the interacting Bose system, which (although similar to collective phase mode branch at small wave-vectors), represents a distinct dynamical mode³². In the composite boson problem the pair excitations and related pair propagator, called $\mathcal{T}(i\Omega, \mathbf{q})$, play an essential role. In the limit of non-zero $Q \equiv (i\Omega, \mathbf{q})$, we refer to this propagator as $\mathcal{T}_{pg}(Q)$, where the subscript pg derives from “pseudogap”. For small Ω and \mathbf{q} , it may be approximated by

$$\mathcal{T}_{pg}(i\Omega, \mathbf{q}) \approx Z/(i\Omega - \Omega_{\mathbf{q}} + i\Gamma_{\mathbf{q}} + \mu_{pair}), \quad (5)$$

where Z is the usual renormalization factor, $i\Omega$ is a bosonic Matsubara frequency, $\Omega_{\mathbf{q}}$ is the dispersion of the finite momentum pair excitations (with $\Omega_{\mathbf{q}=0} = 0$), $\Gamma_{\mathbf{q}}^{-1}$ is the pair excitation lifetime, and μ_{pair} is the associated effective pair “chemical potential” with its value set by the well known (ideal gas) BEC condition

$$\mu_{pair} = 0, \quad \text{for } T \leq T_c. \quad (6)$$

It is this function \mathcal{T}_{pg} , which will be shown in Sec. III, to determine the *fermionic* excitation gap $\Delta(T)$ and chemical potential μ . Moreover, the fermionic excitation gap is related, in turn, to the condition that $\mu_{pair} = 0$ at and below T_c . Quite generally, the presence of incoherent pair excitations blocks the available states for fermions and, thereby, affects the fermion excitation gap. These effects, which occur both above and below T_c , are directly related to particle-hole asymmetry which appears as the system crosses out of the BCS regime.

It should be stressed that within the BCS-BEC crossover picture, the form of \mathcal{T} is highly circumscribed so as to produce the ground state equations, Eqs. (3) and (4). Through these equations the fermionic degrees of freedom play an important role, even at very strong coupling. This constraint can then be used to deduce the function $\Omega_{\mathbf{q}}$. We find that the pairing approximation (discussed in Sec. III below) produces this $T = 0$ description of the fermionic degrees of freedom, and that, as a consequence, for sufficiently small \mathbf{q} , the pair excitation dispersion is given by

$$\Omega_{\mathbf{q}} = \mathbf{q}^2/2M_{\text{pair}} \quad (7)$$

where the pair mass M_{pair} is dependent on g , temperature, density, lattice structure and other materials properties. This dispersion is found to be a consequence of other T-matrix schemes, as well, and takes a similar form above T_c , although there the pairs are not as long lived. Once the pair propagator is characterized, T_c can be obtained either when approached from above or below.

We may now quantify the first point (i) listed above. The deviation between the excitation gap and the order parameter is related to the number of thermally excited finite momentum pair excitations. We define the difference between the excitation gap Δ and order parameter Δ_{sc} as

$$\Delta_{pg}^2 = \Delta^2 - \Delta_{sc}^2, \quad (8)$$

where throughout this paper, Δ_{sc} is taken to be real. The number of (incoherent) pair excitations is given in terms of the pair propagator \mathcal{T}_{pg}

$$\Delta_{pg}^2 = - \sum_Q \mathcal{T}_{pg}(Q) = - \sum_{\mathbf{q}} \int_{-\infty}^{\infty} \frac{d\Omega}{\pi} b(\Omega) \text{Im} \mathcal{T}_{pg}(\Omega, \mathbf{q}), \quad (9)$$

where $b(\Omega)$ is the Bose function and $\mathcal{T}_{pg}(\Omega, \mathbf{q})$ is the analytically continued ($i\Omega \rightarrow \Omega + i0^+$) pair propagator. In the regime of intermediate coupling, where pseudogap effects are apparent, these bosonic excitations act in concert with fermionic excitations¹¹. This is what one expects if there is to be a smooth interpolation between the BCS and BEC limits.

The behavior of Δ_{pg} , Δ and Δ_{sc} is schematically plotted in Fig. 1 in the three different regimes: weak (BCS), intermediate, and strong coupling (nearly BEC) regimes. Below T_c these plots are based on detailed numerical calculations¹⁰, whereas above T_c , where the computations are more difficult¹², on a simple extrapolation procedure.³³

It may be noted that Fig. 1 has a direct analogue in the (Coulomb modulated) phase fluctuation scenario³. The three panels (from top to bottom) would then correspond to progressively decreasing the size of the plasma frequency ω_p . In this phase fluctuation scenario the tuning parameter is ω_p , whereas in the crossover scenario the parameter g sets the scale for the size of Δ_{pg}^2 . It should, thus, be clear that Coulomb-modulated phase fluctuations are not the only way to create an excitation gap which appears above the transition temperature.

It should, finally, be stressed that these incoherent, finite momentum pair excitations, which enter into Δ_{pg} via Eq. (9), are irrelevant in the BCS limit, in accord with Eq. (8) and Fig. 1(a). In that limit the “quasi-particle” assumption implicit in Eq. (5) is invalid and because of both the lack of particle-hole asymmetry and the large damping $\Gamma_{\mathbf{q}}$, the pair excitation spectrum overlaps the particle-particle continuum. One can quantify the reliability of this key approximation. In Fig. 2, using our numerical scheme¹¹, we plot the value Λ of the wave-vector $|\mathbf{q}|$ at which the pair dispersion intersects the continuum states, as a function of coupling g . This corresponds to a measure of the Landau damping of the pair propagator. The shaded region indicates where the incoherent finite momentum pairs represent ill-defined excitations. Outside this shaded region, the assumptions implicit in Eq. (5) should be valid. Related calculations show that $\Delta_{pg}(T_c)/\Delta_{sc}(0)$ is arbitrarily small in the weak coupling limit, so that even if we apply Eq. (5) directly in this limit, pseudogap effects are negligible in the BCS regime.

C. The Strong Coupling Limit: “True” versus Composite Bosons

A first important distinction can be found, between true and composite bosons, at the level of the Leggett ground state. As noted earlier, already at $T = 0$ there appears to be a mix of quasi-ideal and interacting Bose gas character to the strong coupling limit. The gap equation [Eq. (3)] is associated¹⁵ with “noninteracting diatomic molecules”, whereas, the collective mode spectrum^{29,7} reflects an effective boson-boson interaction which relates to the Pauli statistics of the constituent fermions. This is revealed most clearly in jellium models where the AB sound velocity remains finite at infinite g , with an asymptote associated with the residual interactions. Some insight into the origin of these boson-boson effects can be found in Refs. 34 and 35. Indeed, one should be cautious in the use of the phrase effective boson-boson repulsion which, for large g , derives entirely from Fermi statistical effects. Unlike in the interacting Bose system³², where boson-boson interactions need to be separately included in the boson propagator, here the physics associated with the Pauli principle is already accounted for and should not be fed back again to renormalize the dispersion of the composite bosons.

A second important difference arises from the fact that this superconducting ground state corresponds to one in which there is full condensation so that, as in the BCS phase, the condensate fraction $n_0 = n$. By contrast, in a Bose superfluid there is always a depletion of the condensate at $T = 0$, caused by the existence of the boson-boson repulsion.

As a final important difference, we note that the behavior of the pair propagator \mathcal{T} , which must necessarily be consistent with Eqs. (3) and (4), is highly circumscribed and rather different from what one might deduce based on the Bogoliubov model for a Bose liquid³². The fermionic degrees of freedom can never be fully “integrated out”. The fermionic excitation gap Δ and the pair chemical potential $\mu_{pair} = 0$ are, moreover, closely inter-related via, e.g., Eq. (18) below. These effects have no natural counterpart in the Bose liquid (where the fermionic excitation gap is of no consequence). It is, thus, not surprising that in T_c calculations, which are associated with a divergence in \mathcal{T} , a variety of different groups^{16,34,35} find that the strong coupling limit is characterized by a quasi-ideal BEC result

$$T_c = \frac{3.31}{M_{pair}} \left(\frac{n}{2}\right)^{2/3} \quad (10)$$

where M_{pair} is the same pair mass as that which appears in $\Omega_{\mathbf{q}} = \mathbf{q}^2/M_{pair}$ of Eq. (7). Thus, from the perspective of T_c and of the *temperature dependent* gap equations, *the bosons are “free”*, except for the renormalized mass. Related theories have reached rather similar conclusions.^{18,6,36} These conclusions owe their origin to the underlying mean field structure of BCS theory, which is the starting point of the crossover scenario. At a more microscopic level, they appear to be associated with general T-matrix approaches, as is discussed below.

III. SELF-CONSISTENT T-MATRIX APPROXIMATIONS

A. General Results for the Superconducting Phase

In this section we present the self consistency conditions and related gap equations associated with the superconducting state within the broad class of T-matrix-based crossover theories. An important goal of this discussion is to show that Eqs. (5)-(9) are rather general consequences of these schemes when applied below T_c . In these non-perturbative approaches the two-particle Green’s function is expressed in terms of a T-matrix (or pair propagator), $\mathcal{T}(Q)$, which is determined self consistently in terms of the single particle Green’s function. One solves, in effect, three coupled equations for the self energy, T-matrix and chemical potential (via the number equation):

$$\Sigma(K) = G_o^{-1}(K) - G^{-1}(K) = \sum_Q \mathcal{T}(Q) \tilde{G}(Q - K), \quad (11a)$$

$$g = [1 + g\chi(Q)] \mathcal{T}(Q), \quad (11b)$$

$$n = 2 \sum_K G(K). \quad (11c)$$

Here and in what follows we use four-vector notation: $Q \equiv (i\Omega, \mathbf{q})$, $\sum_Q \equiv T \sum_{i\Omega} \sum_{\mathbf{q}}$, etc. The choice of the functions \tilde{G} and pair susceptibility χ varies from one approximation to another. Here we address two different schemes which introduce self consistency at a level beyond the lowest order T-matrix approximation used by NSR,¹⁸ so that our discussion focuses on T-matrix schemes where dressed Green’s functions enter into the self consistency requirements. (a) The first approach, known as the FLEX (or ‘GG’) approximation^{13,35,24} takes $\tilde{G} = G$ with $\chi = \chi^{FLEX}$ where we define

$$\chi^{FLEX}(P) = \sum_K G(K)G(P - K) \quad (12)$$

with the corresponding self energy

$$\Sigma^{FLEX}(K) = \sum_P \mathcal{T}(P)G(P - K) \quad (13)$$

In addition, we study the (b) pairing approximation^{10,11} (or ‘GG_o’ scheme), which sets $\tilde{G} = G_o$ and $\chi = \chi^{pair}$ with

$$\chi^{pair}(P) = \sum_K G(K)G_o(P - K) \quad (14)$$

with the corresponding self energy

$$\Sigma^{pair}(K) = \sum_P \mathcal{T}(P)G_o(P - K) \quad (15)$$

We know of no other literature on the FLEX scheme within the superconducting state (appropriate to a fully three dimensional system). By contrast, above T_c there is considerable literature on the behavior of \mathcal{T} and T_c , which, in the FLEX scheme, have been calculated numerically³⁵ and analytically¹³ by solution of Eqs. (11). As the temperature is lowered, this T-matrix develops a maximum around $Q = 0$ and the transition temperature T_c to the broken symmetry phase is signaled by a pole given by the condition

$$g \mathcal{T}^{-1}(Q = 0; T_c) = 1 + g\chi(Q = 0; T_c, \Delta) = 0. \quad (16)$$

The counterpart of this analysis is considerably more complicated below T_c . The procedure, which we summarize in this section, is an approximation which is chosen to satisfy the following four criteria: (i) It leads to the same transition temperature when approached from below as from above. (ii) It leads directly to a *physical* interpretation of the BCS-BEC crossover scheme as discussed in the previous section and illustrated in Fig. 1. An important, and third criterion which we view as an additional check on the approximations used is that (iii) one should recover the BCS scheme in weak coupling for all $T \leq T_c$ and, finally, (iv) we should recover the Leggett ground state at $T = 0$.

An important premise underlying these crossover schemes is that the particle-particle dominates the particle-hole channel. Without such an assumption one would be forced to evaluate a full 2×2 Nambu matrix Green's function along with a 4×4 T-matrix. A complete self-consistent solution of the resulting set of equations is prohibitively difficult. With the assumption that the particle-particle channel is dominant, one argues that formally the set of Eqs. (11) remains valid below T_c , provided that the T-matrix acquire a singular delta-function component, which describes the ($Q = 0$) Cooper pair condensate in equilibrium, so that

$$\mathcal{T}(Q) = \mathcal{T}_{sc}(Q) + \mathcal{T}_{pg}(Q), \quad (17a)$$

where

$$\mathcal{T}_{sc}(Q) = -\frac{\Delta_{sc}^2}{T} \delta(Q), \quad \text{and} \quad \mathcal{T}_{pg}(Q) = \frac{g}{1 + g\chi(Q)}. \quad (17b)$$

This form for \mathcal{T} guarantees that the regular part \mathcal{T}_{pg} of the T-matrix remains finite for any non-zero $Q = (i\Omega, \mathbf{q})$. Inserting Eqs. (17) into Eq. (11b) and treating separately the delta function contribution and regular terms, one arrives at the following quite general gap equation

$$1 + g\chi(Q = 0; T, \Delta) = 0, \quad T \leq T_c. \quad (18)$$

In our self consistent scheme, the critical temperature T_c can be obtained from Eq. (18) by setting Δ_{sc} , (which is implicitly contained in Δ), to zero. This result coincides precisely with the Thouless criterion of Eq. (16), which is obtained by approaching the transition from above. As a result of the form of Eq. (18), the regular part of the T-matrix $\mathcal{T}_{pg}(Q)$ diverges as $Q \rightarrow 0$; it can be written in the form

$$\mathcal{T}_{pg}(i\Omega, q) = Z/(i\Omega - \Omega_q + i\Gamma_q), \quad T \leq T_c, \quad (19)$$

in accord with Eq. (5). Here $\Gamma_{\mathbf{q}} \rightarrow 0$ as $\mathbf{q} \rightarrow 0$. Equation (18) also leads directly to a microscopic derivation of Eq. (8). The self energy of Eq. (11a) may be decomposed into two terms:

$$\Sigma(K) = \Sigma_{sc}(K) + \Sigma_{pg}(K), \quad (20)$$

where the term associated with the condensate contribution, called \mathcal{T}_{sc} is

$$\Sigma_{sc}(K) = -\Delta_{sc}^2 \tilde{G}(-K). \quad (21)$$

In evaluating the pseudogap contribution to Σ , as a consequence of Eq. (18), the main contribution to the Q sum comes from the small Q region, so that the integral may be approximated by

$$\Sigma_{pg}(K) \approx \tilde{G}(-K) \sum_Q \mathcal{T}_{pg}(Q) = -\Delta_{pg}^2 \tilde{G}(-K). \quad (22)$$

In this way the total self energy is

$$\Sigma(K) \approx -\Delta^2 \tilde{G}(-K), \quad \Delta \equiv \sqrt{\Delta_{sc}^2 + \Delta_{pg}^2}. \quad (23)$$

Here the total excitation gap is to be associated with the parameter Δ , and we see that Eqs. (22) and (23) naturally lead back to the definition of Δ_{pg} which appears in Eq. (8).

There is another way of relating Δ_{pg}^2 to the fluctuations of the pairing field, which leads to a more precise interpretation of Eq. (8). We write the pairing field $\hat{\Delta}_{\mathbf{q}}(t) \equiv |g| \sum_{\mathbf{k}} c_{-\mathbf{k}+\mathbf{q}/2\downarrow}(t) c_{\mathbf{k}+\mathbf{q}/2\uparrow}(t)$, about its mean field value $\langle |\Delta| \rangle \equiv |\langle \hat{\Delta}_{\mathbf{q}=0}(0) \rangle| = \Delta_{sc}$. We define $\langle |\Delta|^2 \rangle \equiv \sum_Q \langle \hat{\Delta}_Q \hat{\Delta}_Q^\dagger \rangle = g^2 \sum_{K, K'} \sum_Q C_2(K, K'; Q)$, where $C_2(K, K'; Q)$ is the proper two-particle correlation function, which in general is not factorizable in the variables K and K' . After some algebra one arrives at

$$\langle |\Delta|^2 \rangle = - \sum_Q \mathcal{T}(Q) [g \chi(Q)]^2. \quad (24)$$

Now, inserting in Eq. (24) the expression for the T-matrix given by Eqs. (17), we obtain

$$\langle |\Delta|^2 \rangle = \Delta_{sc}^2 - \sum_Q \mathcal{T}_{pg}(Q) [g \chi(Q)]^2. \quad (25)$$

Since \mathcal{T}_{pg} is highly peaked about $Q = 0$, the pair susceptibility $\chi(Q)$ on the right hand side in Eq. (25) can be approximated by its $Q = 0$ value. We again make use of the gap equation (18) to write $\sum_Q \mathcal{T}_{pg}(Q) [g \chi(Q)]^2 \approx - \sum_Q \mathcal{T}_{pg}(Q) = \Delta_{pg}^2$. Thus, quite generally

$$\Delta_{pg}^2 = - \sum_Q \mathcal{T}_{pg}(Q) \approx \langle |\Delta|^2 \rangle - \langle |\Delta| \rangle^2. \quad (26)$$

The above discussion is expected to apply to both the FLEX scheme and the pairing approximation. Moreover, on the basis of the behavior above T_c , there is no *a priori* reason to select one approach over the other. However, the latter seems to be preferred if one imposes the third and fourth criteria discussed above.

Indeed, the superconducting state is associated with the self energy of Eq. (21). It can be seen that Σ_{sc} coincides with the BCS self energy if we adopt the pairing approximation so that $\tilde{G} = G_o$. With this result the BCS gap equation follows from Eq. (18):

$$1 + g \sum_Q G(K) G_o(-K) = 1 + g \sum_K \frac{\Delta_{sc}^2}{\omega^2 + E_{\mathbf{k}}^2} = 0. \quad (27)$$

The results of the pairing approximation, at all g , can be summarized simply. This scheme leads to the following equations for the three unknowns Δ , μ , and Δ_{pg}

$$g^{-1} + \sum_{\mathbf{k}} \frac{1 - 2f(E_{\mathbf{k}})}{2E_{\mathbf{k}}} = 0, \quad (28a)$$

where $E_{\mathbf{k}} = \sqrt{\epsilon_{\mathbf{k}}^2 + \Delta^2}$. This equation must be solved self consistently with

$$n = 2 \sum_{\mathbf{k}} \left[v_{\mathbf{k}}^2 + \frac{\epsilon_{\mathbf{k}}}{E_{\mathbf{k}}} f(E_{\mathbf{k}}) \right], \quad (28b)$$

where $v_{\mathbf{k}}^2 = \frac{1}{2}(1 - \epsilon_{\mathbf{k}}/E_{\mathbf{k}})$.

Finally, the decomposition of Δ into Δ_{sc} and Δ_{pg} requires the solution of a third equation, namely Eq. (9), which we repeat here for completeness

$$\Delta_{pg}^2 = - \sum_Q \mathcal{T}_{pg}(Q) = - \sum_{\mathbf{q}} \int_{-\infty}^{\infty} \frac{d\Omega}{\pi} b(\Omega) \text{Im} \mathcal{T}_{pg}(\Omega, \mathbf{q}). \quad (28c)$$

An additional check on the validity of the approximation scheme relates to criterion (iv), that is, the nature of the ground state. It follows from Eq. (28c) that, as a result of the Bose function $b(\Omega)$, quite generally

$$\lim_{T \rightarrow 0} \Delta_{pg} = 0, \quad (29)$$

as is consistent with a physical picture in which Δ_{pg} is associated with classical fluctuations. When this limit is used within the pairing approximation, the ground state which results from Eqs. (28a) and (28b) is the same as that proposed by Leggett [see Eqs. (3) and (4)].

IV. ELECTROMAGNETIC RESPONSE AND COLLECTIVE MODES OF A SUPERCONDUCTOR: BEYOND BCS THEORY

The purpose of this section is to study the gauge invariant (linear) response of a superconductor to an external electromagnetic (EM) field, and obtain the associated collective mode spectrum. Our discussion is generally relevant to complex situations such as those appropriate to the BCS-BEC crossover scenario. An important ingredient of this discussion is establishing the role of particle-hole asymmetry. It should be noted that there are fairly extensive discussions in the literature on the behavior of collective modes within the $T = 0$ crossover scenario^{30,7,29}. Here we review a slightly different formulation^{37,38} which introduces a matrix extension of the Kubo formalism of the normal state. We find that this approach is more directly amenable to extension to finite T , where the pair fluctuation diagrams need to be incorporated.

The definition of the collective modes of a superconductor must be made with some precision. We refer to the underlying Goldstone boson of the charged or uncharged superconductor as the ‘‘AB mode’’, after Anderson³⁹ and Bogoliubov⁴⁰. According to our specific definition, this AB mode appears as a pole structure in the gauge invariant formulations of the electrodynamic response functions, for example, in the density-density correlation function. Early work by Prange⁴¹ referred to this as the ‘‘ghost mode’’ of the neutral system, since this term is not directly affected by the long range Coulomb interaction. By contrast, the normal modes of the charged or uncharged superconductor, which we shall call the ‘‘collective modes’’, involve a coupling between the density, phase, and for the BCS-BEC case, amplitude degrees of freedom. For these, one needs to incorporate a many body theoretic treatment of the particle-hole channel as well. In crossover theories this channel is not as well characterized as is the particle-particle channel.

A. Gauge Invariant EM Response Kernel

In the presence of a weak externally applied EM field, with four-vector potential $A^\mu = (\phi, \mathbf{A})$, the four-current density $J^\mu = (\rho, \mathbf{J})$ is given by

$$J^\mu(Q) = K^{\mu\nu}(Q)A_\nu(Q), \quad (30)$$

where, $Q \equiv q^\mu = (\omega, \mathbf{q})$ is a four-momentum, and $K^{\mu\nu}$ is the EM response kernel which can be written as

$$K^{\mu\nu}(Q) = K_0^{\mu\nu}(Q) + \delta K^{\mu\nu}(Q). \quad (31)$$

Here

$$K_0^{\mu\nu}(\omega, \mathbf{q}) = P^{\mu\nu}(\omega, \mathbf{q}) + \frac{ne^2}{m}g^{\mu\nu}(1 - g^{\mu 0}) \quad (32)$$

is the usual Kubo expression for the electromagnetic response. We define the current-current correlation function $P^{\mu\nu}(\tau, \mathbf{q}) = -i\theta(\tau)\langle [j^\mu(\tau, \mathbf{q}), j^\nu(0, -\mathbf{q})] \rangle$. In the above equation, $g^{\mu\nu}$ is the contravariant diagonal metric tensor, with diagonal elements $(1, -1, -1, -1)$, and n, e and m are the particle density, charge and mass, respectively.

The presence of $\delta K^{\mu\nu}$ in Eq. (31) is due to the perturbation of the superconducting order parameter by the EM field, i.e., to the excitation of the *collective modes* of Δ_{sc} . This term is required to satisfy charge conservation $q_\mu J^\mu = 0$, which requires that

$$q_\mu K^{\mu\nu}(Q) = 0. \quad (33a)$$

Moreover, gauge invariance yields

$$K^{\mu\nu}(Q)q_\nu = 0, \quad (33b)$$

Note that, since $K^{\mu\nu}(-Q) = K^{\nu\mu}(Q)$, the two constraints Eqs. (33) are in fact equivalent.

The incorporation of gauge invariance into a general microscopic theory may be implemented in several ways. Here we do so via a general matrix linear response approach³⁷ in which the perturbation of the condensate is included as additional contributions $\Delta_1 + i\Delta_2$ to the applied external field. These contributions are self consistently obtained (by using the gap equation) and then eliminated from the final expression for $K^{\mu\nu}$. We now implement this procedure. Let $\eta_{1,2}$ denote the change in the expectation value of the pairing field $\hat{\eta}_{1,2}$ corresponding to $\Delta_{1,2}$. For the case of an s -wave pairing interaction $g < 0$, the self-consistency condition $\Delta_{1,2} = -g\eta_{1,2}$ leads to the following equations

$$J^\mu = K^{\mu\nu}A_\nu = K_0^{\mu\nu}A_\nu + R^{\mu 1}\Delta_1 + R^{\mu 2}\Delta_2, \quad (34a)$$

$$\eta_1 = -\frac{\Delta_1}{g} = R^{1\nu} A_\nu + Q_{11}\Delta_1 + Q_{12}\Delta_2, \quad (34b)$$

$$\eta_2 = -\frac{\Delta_2}{g} = R^{2\nu} A_\nu + Q_{21}\Delta_1 + Q_{22}\Delta_2, \quad (34c)$$

where $R^{\mu i}(\tau, \mathbf{q}) = -i\theta(\tau)\langle [j^\mu(\tau, \mathbf{q}), \hat{\eta}_i(0, -\mathbf{q})] \rangle$, with $\mu = 0, \dots, 3$, and $i = 1, 2$; and $Q_{ij}(\tau, \mathbf{q}) = -i\theta(\tau)\langle [\hat{\eta}_i(\tau, \mathbf{q}), \hat{\eta}_j(0, -\mathbf{q})] \rangle$, with $i, j = 1, 2$.

Thus far, the important quantities $K_0^{\mu\nu}$, $R^{\mu i}$ and Q_{ij} are unknowns which contain the details of the appropriate microscopic model. We shall return to these later in Sec. V. The last two of Eqs. (34) can be used to express $\Delta_{1,2}$ in terms of A_ν

$$\Delta_1 = -\frac{\tilde{Q}_{22}R^{1\nu} - Q_{12}R^{2\nu}}{\tilde{Q}_{11}\tilde{Q}_{22} - Q_{12}Q_{21}}A_\nu, \quad (35a)$$

$$\Delta_2 = -\frac{\tilde{Q}_{11}R^{2\nu} - Q_{21}R^{1\nu}}{\tilde{Q}_{11}\tilde{Q}_{22} - Q_{12}Q_{21}}A_\nu, \quad (35b)$$

where $\tilde{Q}_{ii} = 1/g + Q_{ii}$, with $i = 1, 2$. Finally, inserting Eqs. (35) into Eq. (34a) one obtains

$$K^{\mu\nu} = K_0^{\mu\nu} + \delta K^{\mu\nu}, \quad (36a)$$

with

$$\delta K^{\mu\nu} = -\frac{\tilde{Q}_{11}R^{\mu 2}R^{2\nu} + \tilde{Q}_{22}R^{\mu 1}R^{1\nu} - Q_{12}R^{\mu 1}R^{2\nu} - Q_{21}R^{\mu 2}R^{1\nu}}{\tilde{Q}_{11}\tilde{Q}_{22} - Q_{12}Q_{21}}. \quad (36b)$$

As can be seen from the above rather complicated equation, the electromagnetic response of a superconductor involves many different components of the generalized polarizability. Moreover, in the form of Eqs. (36b) it is not evident that the results are gauge invariant. In order to demonstrate gauge invariance and reduce the number of component polarizabilities, we first rewrite $K^{\mu\nu}$ in a way which incorporates the effects of the amplitude contributions via a renormalization of the relevant generalized polarizabilities, i.e.,

$$K^{\mu\nu} = K_0^{\prime\mu\nu} + \delta K^{\prime\mu\nu}, \quad (37a)$$

where

$$K_0^{\prime\mu\nu} = K_0^{\mu\nu} - \frac{R^{\mu 1}R^{1\nu}}{\tilde{Q}_{11}}, \quad (37b)$$

and

$$R^{\prime\mu 2} = R^{\mu 2} - \frac{Q_{12}}{\tilde{Q}_{11}}R^{\mu 2}, \quad \tilde{Q}'_{22} = \tilde{Q}_{22} - \frac{Q_{12}Q_{21}}{\tilde{Q}_{11}}. \quad (37c)$$

In this way we obtain a simpler expression for $\delta K^{\prime\mu\nu}$

$$\delta K^{\prime\mu\nu} = -\frac{R^{\prime\mu 2}R^{\prime 2\nu}}{\tilde{Q}'_{22}}. \quad (38)$$

We now consider a particular (*a priori* unknown) gauge A'^μ in which the current density can be expressed as $J^\mu = K_0^{\prime\mu\nu}A'_\nu$. The gauge transformation⁴² which connects the four-potential A_μ in an arbitrary gauge with A'_μ , i.e., $A'_\mu = A_\mu + i\chi q_\mu$, must satisfy

$$J^\mu = K^{\mu\nu}A_\nu = K_0^{\prime\mu\nu}(A_\nu + i\chi q_\nu). \quad (39)$$

Now invoking charge conservation, one obtains

$$i\chi = -\frac{q_\mu K_0^{\prime\mu\nu}A_\nu}{q_{\mu'} K_0^{\prime\mu'\nu'} q_{\nu'}}, \quad (40)$$

and, therefore,

$$K^{\mu\nu} = K_0^{\prime\mu\nu} - \frac{\left(K_0^{\prime\mu\nu'} q_{\nu'}\right) \left(q_{\nu''} K_0^{\prime\nu''\nu}\right)}{q_{\mu'} K_0^{\prime\mu'\nu'} q_{\nu'}} . \quad (41)$$

The above equation satisfies two important requirements: it is manifestly gauge invariant and, moreover, it has been reduced to a form that depends principally on the four-current-current correlation functions. (The word ‘‘principally’’ appears because in the absence of particle-hole symmetry, there are effects associated with the order parameter amplitude contributions which enter via Eq. (37) and add to the complexity of the calculations). Equation (41) should be directly compared with Eq. (36b). In order for the formulations to be consistent and to explicitly keep track of the conservation laws (33), the following identities must be satisfied:

$$\left(q_{\mu} K_0^{\prime\mu\nu}\right) \tilde{Q}'_{22} = \left(q_{\mu} R^{\prime\mu 2}\right) R^{\prime 2\nu} , \quad (42a)$$

$$\left(K_0^{\prime\mu\nu} q_{\nu}\right) \tilde{Q}'_{22} = R^{\prime\mu 2} \left(R^{\prime 2\nu} q_{\nu}\right) . \quad (42b)$$

These identities may be viewed as ‘‘Ward identities’’ for the superconducting two particle correlation functions³⁸. Any theory which adds additional self energy contributions to the BCS scheme must obey these important equations. We shall return to this issue in Sec. V.

B. The Goldstone Boson or AB Mode

The EM response kernel [cf. Eqs. (37)-(41)] of a superconductor contains a pole structure which is related to the underlying Goldstone boson of the system. Unlike the phase mode component of the collective mode spectrum, this AB mode is independent of Coulomb effects⁴¹. The dispersion of this amplitude renormalized AB mode is given by

$$q_{\mu} K^{\prime\mu\nu} q_{\nu} = 0 . \quad (43)$$

For an isotropic system $K_0^{\prime\alpha\beta} = K_0^{\prime 11} \delta_{\alpha\beta}$, and Eq. (43) can be rewritten as

$$\omega^2 K_0^{\prime 00} + \mathbf{q}^2 K_0^{\prime 11} - 2\omega q_{\alpha} K_0^{\prime 0\alpha} = 0 , \quad (44)$$

with $\alpha = 1, 2, 3$, and in the last term on the LHS of Eq. (44) a summation over repeated Greek indices is assumed. It might seem surprising that from an analysis which incorporates a complicated matrix linear response approach, the dispersion of the AB mode ultimately involves only the amplitude renormalized four-current correlation functions, namely the density-density, current-current and density-current correlation functions. This result is, nevertheless, a consequence of gauge invariance.

At zero temperature $K_0^{\prime 0\alpha}$ vanishes, and the sound-like AB mode has the usual linear dispersion $\omega = \omega_{\mathbf{q}} = c|\mathbf{q}|$ with the ‘‘sound velocity’’ given by

$$c^2 = K_0^{\prime 11} / K_0^{\prime 00} . \quad (45)$$

The equations in this section represent an important starting point for our numerical analysis.

C. General Collective Modes

We may interpret the AB mode as a special type of collective mode which is associated with $A_{\nu} = 0$ in Eqs. (35). This mode corresponds to free oscillations of $\Delta_{1,2}$ with a dispersion $\omega = cq$ given by the solution to the equation

$$\det|Q_{ij}| = \tilde{Q}_{11}\tilde{Q}_{22} - Q_{12}Q_{21} = 0 . \quad (46)$$

More generally, according to Eq. (34a) the collective modes of the order parameter induce density and current oscillations. In the same way as the pairing field couples to the mean field order parameter in the particle-particle channel, the density operator $\hat{\rho}(Q)$ couples to the mean field $\delta\phi(Q) = V(Q)\delta\rho(Q)$, where $V(Q)$ is an effective particle-hole interaction which may derive from the pairing channel or, in a charged superconductor, from the Coulomb interaction. Here $\delta\rho = \langle\hat{\rho}\rangle - \rho_0$ is the expectation

value of the charge density operator with respect to its uniform, equilibrium value ρ_0 . Within our self-consistent linear response theory the field $\delta\phi$ must be treated on an equal footing with $\Delta_{1,2}$, and formally can be incorporated into the linear response of the system by adding an extra term $K_0^{\mu 0}\delta\phi$ to the right hand side of Eq. (34a). The other two Eqs. (34) should be treated similarly. Note that, quite generally, the effect of the ‘‘external field’’ $\delta\phi$ amounts to replacing the scalar potential $A^0 = \phi$ by $\bar{A}^0 = \bar{\phi} = \phi + \delta\phi$. In this way one arrives at the following set of three linear, homogeneous equations for the unknowns $\delta\phi$, Δ_1 , and Δ_2

$$0 = R^{10}\delta\phi + \tilde{Q}_{11}\Delta_1 + Q_{12}\Delta_2, \quad (47a)$$

$$0 = R^{20}\delta\phi + Q_{21}\Delta_1 + \tilde{Q}_{22}\Delta_2, \quad (47b)$$

$$\delta\rho = \frac{\delta\phi}{V} = K_0^{00}\delta\phi + R^{01}\Delta_1 + R^{02}\Delta_2. \quad (47c)$$

The dispersion of the collective modes of the system is given by the condition that the above Eqs. (47) have a nontrivial solution

$$\begin{vmatrix} Q_{11} + 1/g & Q_{12} & R^{10} \\ Q_{21} & Q_{22} + 1/g & R^{20} \\ R^{01} & R^{02} & K_0^{00} - 1/V \end{vmatrix} = 0. \quad (48)$$

In the case of particle-hole symmetry $Q_{12} = Q_{21} = R^{10} = R^{01} = 0$ and, the amplitude mode decouples from the phase and density modes; the latter two are, however, in general coupled.

V. EFFECT OF PAIR FLUCTUATIONS ON THE ELECTROMAGNETIC RESPONSE: SOME EXAMPLES

Once dressed Green’s functions G enter into the calculational schemes, the collective mode polarizabilities (e.g., Q_{22}) and the EM response tensor $K_0^{\mu\nu}$ must necessarily include vertex corrections dictated by the form of the self energy Σ , which depends on the T-matrix \mathcal{T} , which, in turn depends on the form of χ . These vertex corrections are associated with gauge invariance and with the constraints which are summarized in Eqs. (42). It can be seen that these constraints are even more complicated than the Ward identities of the normal state. Indeed, it is relatively straightforward to introduce collective mode effects into the electromagnetic response in a completely general fashion which is required by gauge invariance. This issue was discussed in Sec. IV as well as extensively in the literature^{43,30}. The difficulty is in the implementation. In this section we begin with a discussion of the $T = 0$ behavior where the incoherent pair excitation contributions to the self energy corrections and vertex functions vanish. In this section, we shall keep the symmetry factor $\varphi_{\mathbf{k}}$ explicitly.

A. $T = 0$ Behavior of the AB Mode and Pair Susceptibility

It is quite useful to first address the zero temperature results since there it is relatively simple to compare the associated polarizabilities of the AB mode with that of the pair susceptibility χ . In the presence of particle hole symmetry this collective mode polarizability can be associated with Q_{22} which was first defined in Eq. (34c). In the more general case (which applies away from the BCS limit) Q_{22} must be replaced by a combination of phase and amplitude terms so that it is given by $Q'_{22} = Q_{22} - Q_{12}Q_{21}/Q_{11}$.

We may readily evaluate these contributions in the ground state, where $\Delta_{sc} = \Delta$. The polarizability Q_{22} is given by

$$Q_{22}(Q) = \frac{1}{2} \sum_P [G(-P)G(P-Q) + G(P)G(Q-P) + F^\dagger(P)F^\dagger(P-Q) + F(P)F(P-Q)] \varphi_{\mathbf{p}-\mathbf{q}/2}^2, \quad (49)$$

where

$$G(K) = G_o(K)/[1 + \Delta_{sc}^2 \varphi_{\mathbf{k}}^2 G_o(-K)G_o(K)], \quad (50)$$

and

$$F(P) = \Delta_{sc} \varphi_{\mathbf{p}} G(P)G_o(-P). \quad (51)$$

Now, it can be seen that the pair susceptibility χ in the pairing approximation satisfies

$$\sum_P [G(-P)G(P) + F(P)F(P)] \varphi_{\mathbf{p}}^2 = \sum_P G(P)G_o(-P) \varphi_{\mathbf{p}}^2 = \chi(0) \quad (52)$$

and, moreover, $Q_{12}(0) = Q_{21}(0) = 0$ so that

$$\frac{1}{g} + Q_{22}(0) = \frac{1}{g}[1 + g\chi(0)] = 0. \quad (53)$$

In this way, the AB mode propagator is soft under the same conditions which yield a soft pair excitation propagator $\mathcal{T}_{pg} = g/(1 + g\chi)$, and these conditions correspond to the gap equation Eq. (3). Moreover, it can be seen that $Q'_{22}(Q) = Q'_{22}(-Q)$ so that, upon expanding around $Q = 0$, one has $Q_{22}(Q) = \alpha_{22}\Omega^2 - \beta_{22}q^2$, $Q_{12}(Q) = -Q_{21}(Q) = -i\Omega\alpha_{12}$, and $1/g + Q_{11}(Q) = 1/g + \alpha_{11}$, where

$$\begin{aligned} \alpha_{22} &= \sum_{\mathbf{k}} \frac{\varphi_{\mathbf{k}}^2}{8E_{\mathbf{k}}^3}, \\ \beta_{22} &= \frac{1}{d} \sum_{\mathbf{k}} \frac{1}{8E_{\mathbf{k}}^3} \left[\varphi_{\mathbf{k}}^2 (\vec{\nabla}\epsilon_{\mathbf{k}})^2 - \frac{1}{4} (\vec{\nabla}\epsilon_{\mathbf{k}}^2) \cdot (\vec{\nabla}\varphi_{\mathbf{k}}^2) \right], \\ \alpha_{12} &= \sum_{\mathbf{k}} \frac{\epsilon_{\mathbf{k}}}{4E_{\mathbf{k}}^3} \varphi_{\mathbf{k}}^2, \\ \alpha_{11} &= \sum_{\mathbf{k}} \frac{\epsilon_{\mathbf{k}}^2}{2E_{\mathbf{k}}^3} \varphi_{\mathbf{k}}^2, \end{aligned} \quad (54)$$

where d denotes the dimensionality of the system. Thus, one obtains

$$c^2 = \frac{\beta_{22}}{\alpha_{22} + \frac{\alpha_{12}^2}{1/g + \alpha_{11}}}. \quad (55)$$

At weak coupling in 3D, where one has particle-hole symmetry, $\alpha_{12} = 0$, the amplitude and the phase modes decouple. This leads to the well known result $c = v_F/\sqrt{3}$. More generally, for arbitrary coupling strength g , these equations yield results equivalent to those in the literature^{29,7,30}, as well as those derived from the formalism of Sec. IV.B. Finally, it should be noted that, since both Eqs. (41) and (38) have the same poles, the condition $Q'_{22}(Q) = 0$ yields the same AB mode dispersion as that determined from Eq. (43). This is a consequence of gauge invariance.

B. AB Mode at Finite Temperatures

We now turn to finite temperatures where there is essentially no prior work on the collective mode behavior in the crossover scenario. At the level of BCS theory (and in the Leggett ground state) the extended ‘‘Ward identities’’ of Eqs. (42) can be explicitly shown to be satisfied. Presumably they are also obeyed in the presence of impurities, as, for example, in the scheme of Ref. 37. However, in general, it is difficult to go beyond these simple cases in computing all components of the matrix response function. Fortunately, the calculation of the AB mode is somewhat simpler. It reduces to a solution of Eq. (44), which, *in the presence of particle-hole symmetry*, involves a computation of only the electromagnetic response kernel: the density-density, density-current and current-current correlation functions.

It is the goal of this section to compute these three response functions within the ‘‘pairing approximation’’ to the T-matrix. Our work is based on the normal state approach of Patton²⁷ and the associated diagrams are shown in Fig. 3. Because full Green’s functions G appear in place of G_o (as indicated by the heavy lines) these diagrams are related to but different from their counterparts studied by Aslamazov and Larkin and by Maki and Thompson²⁷. This diagram scheme forms the basis for calculations published by our group^{10,16} of the penetration depth within the BCS-BEC crossover scheme.

Here we make one additional assumption. We treat the amplitude renormalizations which appear in Eqs. (37), only approximately since these contributions introduce a variety of additional correlation functions, which must be calculated in a consistent fashion, so as to satisfy Eqs. (42). Because the amplitude mode is gapped, at least at low T , we can approximate these amplitude renormalizations by their $T = 0$ counterparts, which are much simpler to deduce.

The three electromagnetic correlation functions reduce to a calculation of $P^{\mu\nu}$, which can be written as

$$P^{\mu\nu}(Q) = 2 \sum_K \lambda^\mu(K, K - Q) G(K) G(K - Q) \Lambda^\nu(K, K - Q), \quad (56)$$

where $\lambda(K, K - Q) = (1, \frac{\partial \epsilon_{\mathbf{k}-\mathbf{q}/2}}{\partial \mathbf{k}})$ and $\Lambda(K, K - Q) = \lambda(K, K - Q) + \delta\Lambda_{sc}(K, K - Q) + \delta\Lambda_{pg}(K, K - Q)$ are the bare and full vertices, respectively.

To evaluate the vertex function Λ^μ we decompose it into a pseudogap contribution Λ_{pg} and a superconducting contribution Λ_{sc} . (The latter can be regarded as the Gor'kov “ F ” function contribution, although we do not use that notation here). The pseudogap contribution comes from a sum of Maki-Thompson (MT) and Aslamazov-Larkin (AL_{1,2}) type of diagrams [see Fig. 3(b)]. Since these vertex corrections can be obtained from a proper vertex insertion to the self energy, it follows that there is a cancellation between these various terms which simplifies the algebra. This cancellation is shown in more detail in Appendix A. Following the analysis in this Appendix, the sum of both pg and sc contributions is given by

$$\begin{aligned} \delta\Lambda^\mu(K, K-Q) \approx & -(\Delta_{sc}^2 - \Delta_{pg}^2)\varphi_{\mathbf{k}}\varphi_{\mathbf{k}-\mathbf{q}}G_0(-K)G_0(Q-K)\lambda^\mu(Q-K, -K) \\ & -\Delta_{pg}^2G_0(-K)\frac{\partial\varphi_{\mathbf{k}-\mathbf{q}/2}^2}{\partial k_\mu}, \end{aligned} \quad (57)$$

where use has been made of the fact that $\mathcal{T}_{pg}(Q)$ is highly peaked at $Q=0$, and that $\Delta_{pg}^2 \equiv -\sum_Q \mathcal{T}_{pg}(Q)$.

The AB mode dispersion involves the sum of three terms which enter into Eqs. (43) and (44). We next substitute Eqs. (57) into Eq. (56). After performing the Matsubara frequency summation, and analytically continuing $i\Omega \rightarrow \Omega + i0^+$, we obtain for small Ω and \mathbf{q}

$$\begin{aligned} q_\mu K_0^{\mu\nu} q_\nu = & \mathbf{q} \cdot \left(\frac{\overleftrightarrow{n}}{m} + \overleftrightarrow{\mathbf{P}} \right) \cdot \mathbf{q} - 2\Omega\mathbf{q} \cdot \mathbf{P}_0 + \Omega^2 P_{00} \\ = & \frac{2}{d}q^2 \sum_{\mathbf{k}} \frac{\Delta_{sc}^2}{E_{\mathbf{k}}^2} \left[\frac{1-2f(E_{\mathbf{k}})}{2E_{\mathbf{k}}} + f'(E_{\mathbf{k}}) \right] \left[\varphi_{\mathbf{k}}^2 (\vec{\nabla}\epsilon_{\mathbf{k}})^2 - \frac{1}{4}(\vec{\nabla}\epsilon_{\mathbf{k}}^2) \cdot (\vec{\nabla}\varphi_{\mathbf{k}}^2) \right] \\ & - 2\Omega^2 \sum_{\mathbf{k}} \left\{ \frac{\Delta_{sc}^2\varphi_{\mathbf{k}}^2}{E_{\mathbf{k}}^2} \left[\frac{1-2f(E_{\mathbf{k}})}{2E_{\mathbf{k}}} + f'(E_{\mathbf{k}}) - f'(E_{\mathbf{k}}) \frac{\Omega^2 - (\mathbf{q} \cdot \vec{\nabla}\epsilon_{\mathbf{k}})^2 - \Delta^2(\mathbf{q} \cdot \vec{\nabla}\varphi_{\mathbf{k}})^2}{\Omega^2 - (\mathbf{q} \cdot \vec{\nabla}E_{\mathbf{k}})^2} \right] \right. \\ & \left. + \frac{\Delta_{pg}^2}{4E_{\mathbf{k}}^2} f'(E_{\mathbf{k}}) \frac{(\mathbf{q} \cdot \nabla\epsilon_{\mathbf{k}}^2)(\mathbf{q} \cdot \vec{\nabla}\varphi_{\mathbf{k}}^2) + \Delta^2(\mathbf{q} \cdot \vec{\nabla}\varphi_{\mathbf{k}}^2)^2}{\Omega^2 - (\mathbf{q} \cdot \vec{\nabla}E_{\mathbf{k}})^2} \right\}, \end{aligned} \quad (58)$$

where $f(E)$ is the Fermi function. Because Eq. (58) is ill-behaved for long wavelengths and low frequencies, in order to calculate the AB mode velocity one needs to take the appropriate limit $\Omega = cq \rightarrow 0$. By contrast, the calculation of the London penetration depth first requires to set $\Omega = 0$ (static limit), and then $\mathbf{q} \rightarrow 0$. The superfluid density n_s can be calculated from the coefficient of the q^2 term in Eq. (58), (see, also Eq. (B1) for $Q=0$). Finally, the AB mode “sound” velocity $c = \Omega/q$, in the absence of the amplitude renormalization, can be obtained by solving $q_\mu K_0^{\mu\nu} q_\nu = 0$.

In the absence of the pseudogap (i.e., when $\Delta_{sc} = \Delta$) the last term inside $\{\dots\}$ in Eq. (58) drops out, and the resulting analytical expression reduces to the standard BCS result⁴⁴, which at $T=0$ has the relatively simple form

$$q_\mu K_0^{\mu\nu} q_\nu = \frac{q^2}{d} \sum_{\mathbf{k}} \frac{\Delta_{sc}^2}{E_{\mathbf{k}}^3} \left[\varphi_{\mathbf{k}}^2 (\vec{\nabla}\epsilon_{\mathbf{k}})^2 - \frac{1}{4}(\vec{\nabla}\epsilon_{\mathbf{k}}^2) \cdot (\vec{\nabla}\varphi_{\mathbf{k}}^2) \right] - \Omega^2 \sum_{\mathbf{k}} \frac{\Delta_{sc}^2\varphi_{\mathbf{k}}^2}{E_{\mathbf{k}}^3}. \quad (59)$$

At finite T , the AB mode becomes damped, and the real and imaginary parts of the sound velocity have to be calculated numerically. Although, the algebra is somewhat complicated, it can be shown that the AB mode satisfies $c \rightarrow 0$ as $T \rightarrow T_c$, as expected.

VI. NUMERICAL RESULTS: ZERO AND FINITE TEMPERATURES

In this section we summarize numerical results obtained for the AB mode velocity c associated with the electromagnetic response kernel, as obtained by solving Eqs. (43) and (44). We also briefly discuss the behavior for the $T=0$ phase mode velocity v_ϕ which results from the coupling to density fluctuations, as well [see Eq. (48)]. The former, which has physical implications for the behavior of the dielectric constant^{41,38}, is the more straightforward to compute, because it does not require any new approximations associated with the effective interactions V in the particle-hole channel. The analysis of this section provides information about the nature of the “quasi-ideal” Bose gas limit, which we address via plots of the infinite g asymptote of the AB mode, called c_∞ . It also helps to clarify how pair fluctuations contribute, at finite temperatures, to the collective mode dispersion. Our $T=0$ calculations are based on the Leggett ground state which corresponds to that of the pairing approximation as well. At finite T , we numerically evaluate the AB sound dispersion from Eq. (58), obtained within the framework of the pairing approximation.

In Fig. 4 we plot the zero temperature value of c as a function of the dimensionless coupling strength g/g_c , where $g_c = -4\pi/mk_0$ is the critical value of the coupling above which bound pairs are formed in vacuum. Here we consider a 3D jellium

model at three different electron densities, which are parameterized via k_0/k_F . The most interesting feature of these and related curves is shown in the inset where we plot the asymptotic limit for each value of density or, equivalently, k_0 . This numerically obtained asymptote reflects the *effective* residual boson-boson interactions in the “quasi-ideal” Bose gas limit, and is close to the value calculated in Ref. 31 whose functional dependence is given by $c_\infty/v_F \propto \sqrt{k_F/k_0}$ or, equivalently, $c_\infty \propto \sqrt{n/k_0}$. Interpreting the physics as if the system were a true interacting Bose system, one would obtain an effective interaction $U(0) \approx 3\pi^2/mk_0$, *independent of g in the strong coupling limit*. As expected, these inter-boson interactions come exclusively from the underlying fermion character of the system, and can be associated with the repulsion between the fermions due to the Pauli principle. All of this is seen most directly³⁴ by noting that the behavior displayed in the inset can be interpreted in terms of the effective scattering length of the bosons a_B which is found to be twice that of the fermions a_F in the strong coupling limit. Effects associated with the coupling constant g are, thus, entirely incorporated into making bosons out of a fermion pair, and are otherwise invisible.

The same calculations are repeated in Fig. 5 for a tight binding lattice bandstructure at $T = 0$. Figure 5(a) plots the sound velocity for different densities n , as a function of the coupling constant; the behavior of the large g limit is shown in Fig. 5(b) as a function of density for a fixed g . Near half filling, where there is particle-hole symmetry, the amplitude contributions are irrelevant and the large g limit for c , which follows from Eq. (59), is $c = \sqrt{2}t$, where t is the hopping integral. At low n the AB velocity varies as \sqrt{n} , which is consistent with the results shown above for jellium. In both cases the behavior again reflects the underlying fermionic character, since it is to be associated with a Pauli principle induced repulsion between bosons. Unlike in the jellium case, where c approaches a finite asymptote as g increases, here c vanishes asymptotically due to the increase of the pair mass associated with lattice effects.^{18,16} For completeness, we also show, as an inset in Fig. 5(b), the behavior of v_ϕ , where we have used the RPA approximation to characterize the parameter V in the particle-hole channel. This approximation is in the spirit of previous work by Belkhir and Randeria²⁹, although it cannot be readily motivated at sufficiently large g .

Finally, in Fig. 6 we plot the temperature dependence of the AB mode velocity (both real and imaginary parts), for moderately strong coupling (solid lines) and the BCS limit (dashed lines). For the former, our curves stop somewhat below T_c , since close to the critical temperature, inaccuracies are introduced by our neglect of the temperature dependence of the amplitude mode contributions to c . It should be noted that the transition from a finite to zero value for the “sound” velocity appears to be rather abrupt in the vicinity of T_c , the stronger the coupling. This figure suggests that the AB mode velocity reflects the same transition temperature T_c as is computed via the excited pair propagator, or T-matrix. This represents an important self consistency check on the present formalism.

VII. CONCLUSIONS

This paper deals with the fairly complex issues of pair fluctuations, collective modes and gauge invariance in a BCS Bose-Einstein crossover scenario. A starting point for our approach is the Leggett ground state, which imposes rather strong constraints on the nature of the physics of fermions and composite bosons. The fermion degrees of freedom are always present through the self consistency conditions and can never be fully integrated out. Not only are these fermion pairs different from true bosons, but they represent a very special type of composite boson. They behave rather specifically, in correspondence with the underlying structure of the BCS state. Even at $T = 0$ one can see from previous work on the BCS-BEC crossover, that these constraints lead to a mix of ideal Bose gas¹⁵ and non-ideal²⁹ Bose liquid behavior. This mirrors some of the effects of BCS theory, in which the system undergoes a form of Bose condensation with a full condensate fraction $n_0/n = 1$, at $T = 0$. Nevertheless, a BCS superconductor has a sound-like collective (phase) mode which is intimately associated with its superconductivity. Moreover, as is discussed in Sec. V.A, it is instructive to contrast the polarizability associated with the phase mode, called $Q'_{22}(Q)$, with the pair susceptibility $\chi(Q)$. These two modes correspond to distinct dynamical branches, although both become soft at $\mathbf{q} = \mathbf{0}$ under the same conditions. The softness of the former is naturally associated with the Goldstone boson and the latter with a vanishing chemical potential for pairs: $\mu_{pair} = 0$.

A central physics theme of this paper is reflected in Fig. 1. The crossover problem introduces an important new parameter Δ_{pg} which characterizes the excited states of a non-BCS superconductor. As a result, there are three coupled equations to be satisfied for Δ_{pg} , Δ and μ , at finite T , in contrast to zero temperature crossover theories where there are only two. This new parameter is a measure of the difference between the excitation gap and the superconducting order parameter. One can also arrive at a picture which is similar to Fig. 1 within the Coulomb-modulated phase fluctuation scenario³. What is different here is the “tuning parameter”, which corresponds to the coupling strength g in the crossover picture, and the plasma frequency ω_p in the phase fluctuation scenario.

One may summarize our results by asking the following series of questions, which our paper raises and answers.

Is there any precedent for soft modes other than Goldstone bosons?

Yes. In the present paper we find that a vanishing value for the pair chemical potential μ_{pair} below T_c leads to a soft mode corresponding to incoherent, finite momentum pair excitations. These excitations are analogous to the “particle” excitations in

the case of the neutral Bose liquid. Moreover, for the Bose liquid, this branch is also soft and always different (except at zero wavevector) from the Goldstone boson. However, in the true Bose system the two branches have the same slope at $\mathbf{q} = 0$.

Should the T-matrix \mathcal{T} be renormalized so as to yield the sound mode dispersion at small wave-vectors, as in a Bose liquid? With this renormalization \mathcal{T} would then be similar to its Bose liquid counterpart³² and in this way the pair excitation dispersion $\Omega_{\mathbf{q}}$ at small wavevectors would be linear in \mathbf{q} . We answer this question by noting that the fermion degrees of freedom strongly constrain \mathcal{T} so that the composite boson system is different from the Bose liquid. As a consequence the proposed renormalization seems problematical for two reasons. Adding in this collective mode effect associated with the Bose liquid is equivalent to including boson-boson interactions. In the present composite boson case, these boson-boson interactions derive from fermionic degrees of freedom, i.e., the Pauli principle, which have already been accounted for in our calculations of \mathcal{T} . It is not clear why these boson-boson interactions should then be included yet a second time. Secondly, once there is a renormalization of \mathcal{T} , this will change the ground state gap equation and corresponding constraint on the fermionic chemical potential μ , associated with the changed fermionic self energy Σ . Moreover, this renormalization will, presumably, introduce an unphysical incomplete condensation in the ground state, like its counterpart in the Bose liquid. In summary, the composite boson system is considerably different from the true boson system, because the underlying fermionic constraints (through Δ , μ) can never be ignored.

What about Coulomb renormalizations of the pair propagator?

If Coulomb interactions were included, it would follow, if the analogy were appropriate, that the pair fluctuation mode would then be gapped. This would again compromise the self consistent conditions which must be satisfied from the fermionic perspective (i.e., Δ and μ) in the Leggett ground state. Indeed, within the BCS formalism (as well as in the Leggett ground state) long range Coulomb interactions do not enter in an important way to change the gap equation structure, but rather they principally affect the collective modes. It is for this reason that we argued earlier that Coulomb effects are presumed to be already included in the pairing interaction. It should be recalled that at large g , we have seen that essentially all signs of the two body (g dependent) fermion-fermion interaction are absent in the effective boson-boson interaction.

Does this paper in any way change the way we think about BCS theory? Absolutely not. BCS theory appears as a special case in the weak coupling g , particle-hole symmetric limit of our more general approach. When we study pair excitations in this limit, we find they are greatly damped at all wavevectors q , and it makes no sense to talk about them. In this way $\Delta_{pg}(T_c)/\Delta_{sc}(0)$ is vanishingly small in the BCS limit.

To what extent are the results of this paper limited by the T matrix approximation? The T-matrix approximation seems to be intimately connected to the physics of the crossover scenario. This scheme represents, in some sense, a truncation of the interactions at a pair-wise level. This truncation, which appears to generate a quasi-ideal Bose gas character to the composite boson system, mirrors the behavior of the well established ground state. This approach might not be suitable for other composite boson scenarios, which do not evolve directly from the BCS phase. Nevertheless, these crossover schemes provide a useful way of learning about composite boson systems in general. Moreover, they provide valuable insights about how to extend BCS theory slightly, without abandoning it altogether, and in this way to address a large class of short coherence length, but otherwise conventional, superconductors.

ACKNOWLEDGMENTS

We are very grateful to Gene Mazenko, Andrei Varlamov and Paul Wiegmann for useful discussions and to Igor Kulik for helpful communications. This work was supported by grants from the National Science Foundation through the Science and Technology Center for Superconductivity under Grant No. DMR 91-20000 and through the MRSEC under Grant No. DMR 9808595, 5-43030.

APPENDIX A: EVALUATION OF THE VERTEX CORRECTIONS

In this appendix we demonstrate an explicit cancellation between the Maki-Thompson (MT) and Aslamazov-Larkin (AL) diagrams of Fig. 3. In this way we prove that the contribution to the vertex correction $\delta\Lambda$ from the superconducting order parameter is given by the Maki-Thompson diagram, and the pseudogap contribution $\delta\Lambda_{pg}$ comes from Maki-Thompson (MT) and Aslamazov-Larkin (AL) diagrams. It is easy to demonstrate a cancellation between the MT diagram and the AL diagrams, which will greatly simplify the calculations. In general, we have

$$\delta\Lambda_{pg}^{\mu}(K, K - Q)q_{\mu} = -(MT)_{pg} + \sum_P \mathcal{T}_{pg}(P)G_0(P - K)\frac{\partial\varphi_{\mathbf{k}-\mathbf{P}/2-\mathbf{q}/2}^2}{\partial\mathbf{k}} \cdot \mathbf{q}, \quad (\text{A1})$$

where $(MT)_{pg}$ refers to the MT diagram contribution, and $\mathcal{T}_{pg}(Q \neq 0)$ is the T matrix or pair propagator.

To prove this cancellation, we notice that the vertex corrections in the (four-)current-current correlation functions can be obtained from proper vertex insertions in the single particle Green's functions in the self-energy diagram. In the pairing approximation (G_oG scheme) we have

$$\Sigma_{pg}(K) = \sum_L \mathcal{T}_{pg}(K+L)G_0(L)\varphi_{(K-L)/2}^2, \quad (\text{A2})$$

where L is the four-momentum of the fermion loop, this procedure leads to one Maki-Thompson diagram and two Aslamazov-Larkin diagrams.

Obviously, L in the Eq. (A2) is a dummy variable so that its variation does not change $\Sigma(K)$, namely,

$$\begin{aligned} 0 &= \sum_L \left[\mathcal{T}_{pg}((K+L+\Delta L)G_0(L+\Delta L)\varphi_{(K-L-\Delta L)/2}^2 - \mathcal{T}_{pg}((K+L)G_0(L)\varphi_{(K-L)/2}^2) \right] \\ &= \sum_L \left\{ [\mathcal{T}_{pg}(K+L+\Delta L) - \mathcal{T}_{pg}(K+L)] G_0(L+\Delta L)\varphi_{(K-L-\Delta L)/2}^2 \right. \\ &\quad \left. + \mathcal{T}_{pg}(K+L) [G_0(L+\Delta L) - G_0(L)] \varphi_{(K-L-\Delta L)/2}^2 + \mathcal{T}_{pg}(K+L)G_0(L) \left[\varphi_{(K-L-\Delta L)/2}^2 - \varphi_{(K-L)/2}^2 \right] \right\} \quad (\text{A3}) \end{aligned}$$

Using $G(K)G^{-1}(K) = 1$, we obtain

$$\begin{aligned} G(K+\Delta K) - G(K) &= -G(K)[G^{-1}(K+\Delta K) - G^{-1}(K)]G(K+\Delta K) \\ &= -G(K)\Lambda_\mu(K+\Delta K, K)G(K)\Delta K^\mu, \quad (\text{A4a}) \end{aligned}$$

where $G^{-1}(K+\Delta K) - G^{-1}(K) \approx \Lambda_\mu(K+\Delta K, K)\Delta K^\mu$ is the full vertex. Similarly, we have

$$\begin{aligned} G_0(K+\Delta K) - G_0(K) &= -G_0(K)[G_0^{-1}(K+\Delta K) - G_0^{-1}(K)]G_0(K+\Delta K) \\ &= -G_0(K)\lambda_\mu(K+\Delta K, K)G_0(K)\Delta K^\mu, \quad (\text{A4b}) \end{aligned}$$

where $G_0^{-1}(K+\Delta K) - G_0^{-1}(K) \approx \lambda_\mu(K+\Delta K, K)\Delta K^\mu$ is the bare vertex, and $\lambda^\mu(K+\Delta K, K) = (1, \vec{\nabla}_{\mathbf{k}}\epsilon_{\mathbf{k}+\Delta\mathbf{k}/2})$.

Equations (A4) correspond to the vertex insertions diagrammatically along the full and bare Green's functions, respectively.

Using $\mathcal{T}_{pg}(K+L) = g/[1 + g\chi(K+L)]$, we obtain

$$\mathcal{T}_{pg}(K+L+\Delta L) - \mathcal{T}_{pg}(K+L) = -\mathcal{T}_{pg}(K+L+\Delta L)[\chi(K+L+\Delta L) - \chi(K+L)]\mathcal{T}_{pg}(K+L) \quad (\text{A5})$$

Writing $\chi(K+L) = \sum_{L'} G(L')G_0(K+L-L')\varphi_{L'-(K+L)/2}^2$, we have

$$\begin{aligned} \chi(K+L+\Delta L) - \chi(K+L) &= \sum_{L'} G(L') \left\{ [G_0(K+L-L'+\Delta L) - G_0(K+L-L')] \varphi_{L'-(K+L+\Delta L)/2}^2 \right. \\ &\quad \left. + G_0(K+L-L') \left[\varphi_{L'-(K+L+\Delta L)/2}^2 - \varphi_{L'-(K+L)/2}^2 \right] \right\} \quad (\text{A6}) \end{aligned}$$

On the other hand, writing $\chi(K+L) = \sum_{L'} G(K+L-L')G_0(L')\varphi_{(K+L)/2-L'}^2$, we get

$$\begin{aligned} \chi(K+L+\Delta L) - \chi(K+L) &= \sum_{L'} \left\{ [G(K+L-L'+\Delta L) - G(K+L-L')] G_0(L')\varphi_{(K+L+\Delta L)/2-L'}^2 \right. \\ &\quad \left. + G(L')G_0(K+L-L') \left[\varphi_{L'-(K+L-\Delta L)/2}^2 - \varphi_{L'-(K+L)/2}^2 \right] \right\} \quad (\text{A7}) \end{aligned}$$

Combining Eq. (A6) and Eq. (A7), we obtain to the first order of ΔL

$$\begin{aligned} \chi(K+L+\Delta L) - \chi(K+L) &= \frac{1}{2} \sum_{L'} \left\{ G(L') [G_0(K+L-L'+\Delta L) - G_0(K+L-L')] \varphi_{L'-(K+L+\Delta L)/2}^2 \right. \\ &\quad \left. + [G(K+L-L'+\Delta L) - G(K+L-L')] G_0(L')\varphi_{L'-(K+L+\Delta L)/2}^2 \right\}, \quad (\text{A8}) \end{aligned}$$

where we have assumed in general $\varphi_K^2 = \varphi_{-K}^2$. Substituting Eq. (A8) and Eq. (A5) into Eq. (A3), we obtain

$$\begin{aligned}
0 = & -\frac{1}{2} \sum_{LL'} \mathcal{T}_{pg}(K+L+\Delta L) \mathcal{T}_{pg}(K+L) \left\{ G(L') [G_0(K+L-L'+\Delta L) - G_0(K+L-L')] \varphi_{L'-(K+L+\Delta L)/2}^2 \right. \\
& + [G(K+L-L'+\Delta L) - G(K+L-L')] G_0(L') \varphi_{L'-(K+L+\Delta L)/2}^2 \left. \right\} G_0(L+\Delta L) \varphi_{(K-L-\Delta L)/2}^2 \\
& + \sum_L \mathcal{T}_{pg}(K+L) [G_0(L+\Delta L) - G_0(L)] \varphi_{(K-L-\Delta L)/2}^2 \\
& + \sum_L \mathcal{T}_{pg}(K+L) G_0(L) \left[\varphi_{(K-L-\Delta L)/2}^2 - \varphi_{(K-L)/2}^2 \right]
\end{aligned} \tag{A9}$$

Comparing this with the analytical expressions corresponding to the diagrams in Fig. 3, it is easy to identify the first two terms as the two AL diagrams (which we denote by AL_1 and AL_2) and the third one with the MT diagram for the pseudogap vertex corrections. Therefore,

$$\frac{1}{2} [(AL_1) + (AL_2)] + (MT)_{pg} + \sum_L \mathcal{T}_{pg}(K+L) G_0(L) \left[\varphi_{(K-L-\Delta L)/2}^2 - \varphi_{(K-L)/2}^2 \right] = 0 \tag{A10}$$

Finally, we have

$$\begin{aligned}
\delta\Lambda_{pg}^\mu(K, K-\Delta L)\Delta L_\mu &= (AL_1) + (AL_2) + (MT)_{pg} \\
&= -(MT)_{pg} - 2 \sum_L \mathcal{T}_{pg}(K+L) G_0(L) \frac{\partial \varphi_{(K-L-\Delta L)/2}^2}{\partial L} \cdot \Delta L
\end{aligned} \tag{A11}$$

Changing variables $K+L \rightarrow P$, $\Delta L \rightarrow Q$ leads to Eq. (A1).

The two contributions which enter Eq. (57) result from adding the superconducting gap and pseudogap terms which are given respectively by

$$\delta\Lambda_{sc}(K, K-Q) = -\Delta_{sc}^2 \varphi_{\mathbf{k}} \varphi_{\mathbf{k}-\mathbf{q}} G_0(-K) G_0(Q-K) \lambda(Q-K, -K), \tag{A12a}$$

and

$$\begin{aligned}
\delta\Lambda_{pg}^\mu(K, K-Q) &= - \sum_P \mathcal{T}_{pg}(P) \varphi_{\mathbf{k}-\mathbf{p}/2} \varphi_{\mathbf{k}-\mathbf{q}-\mathbf{p}/2} G_0(P-K) G_0(P+Q-K) \lambda^\mu(P+Q-K, P-K) \\
&+ \sum_P \mathcal{T}_{pg}(P) G_0(P-K) \frac{\partial \varphi_{\mathbf{k}-\mathbf{p}/2-\mathbf{q}/2}^2}{\partial k_\mu},
\end{aligned} \tag{A12b}$$

APPENDIX B: FULL EXPRESSIONS FOR THE CORRELATION FUNCTIONS \vec{P} , \mathbf{P}_0 AND P_{00}

It is useful here to write down the component contributions to the different correlation functions in the electromagnetic response. After adding the superconducting and pseudogap contributions one finds for the current-current correlation function

$$\begin{aligned}
\frac{\overleftrightarrow{n}}{m} + \overleftrightarrow{\mathbf{P}} &= 2 \sum_{\mathbf{k}} \frac{\Delta_{sc}^2}{E_{\mathbf{k}}^2} \left[\frac{1-2f(E_{\mathbf{k}})}{2E_{\mathbf{k}}} + f'(E_{\mathbf{k}}) \right] \left[\varphi_{\mathbf{k}}^2(\vec{\nabla}\epsilon_{\mathbf{k}})(\vec{\nabla}\epsilon_{\mathbf{k}}) - \frac{1}{4}(\vec{\nabla}\epsilon_{\mathbf{k}}^2)(\vec{\nabla}\varphi_{\mathbf{k}}^2) \right] \\
&- 2 \sum_{\mathbf{k}} f'(E_{\mathbf{k}}) \frac{\Omega^2}{\Omega^2 - (\mathbf{q} \cdot \vec{\nabla}E_{\mathbf{k}})^2} (\vec{\nabla}\epsilon_{\mathbf{k}})(\vec{\nabla}\epsilon_{\mathbf{k}}) \\
&+ \sum_{\mathbf{k}} \frac{\Delta_{pg}^2}{E_{\mathbf{k}}^2} f'(E_{\mathbf{k}}) \frac{\Omega^2}{\Omega^2 - (\mathbf{q} \cdot \vec{\nabla}E_{\mathbf{k}})^2} \left[\varphi_{\mathbf{k}}^2(\vec{\nabla}\epsilon_{\mathbf{k}})(\vec{\nabla}\epsilon_{\mathbf{k}}) - \frac{1}{4}(\vec{\nabla}\epsilon_{\mathbf{k}}^2)(\vec{\nabla}\varphi_{\mathbf{k}}^2) \right],
\end{aligned} \tag{B1}$$

and for the current-density correlation function

$$\mathbf{P}_0 = -2\Omega \sum_{\mathbf{k}} \frac{\epsilon_{\mathbf{k}}}{E_{\mathbf{k}}} f'(E_{\mathbf{k}}) \frac{\mathbf{q} \cdot \vec{\nabla}E_{\mathbf{k}}}{\Omega^2 - (\mathbf{q} \cdot \vec{\nabla}E_{\mathbf{k}})^2} \vec{\nabla}\epsilon_{\mathbf{k}}, \tag{B2}$$

and finally for the density-density correlation function

$$P_{00} = -2 \sum_{\mathbf{k}} \frac{\Delta_{sc}^2 \varphi_{\mathbf{k}}^2}{E_{\mathbf{k}}^2} \left[\frac{1 - 2f(E_{\mathbf{k}})}{2E_{\mathbf{k}}} + f'(E_{\mathbf{k}}) \right] + 2 \sum_{\mathbf{k}} f'(E_{\mathbf{k}}) \frac{\Omega^2 \Delta_{sc}^2 \varphi_{\mathbf{k}}^2 - E_{\mathbf{k}}^2 (\mathbf{q} \cdot \vec{\nabla} E_{\mathbf{k}})^2}{E_{\mathbf{k}}^2 \left[\Omega^2 - (\mathbf{q} \cdot \vec{\nabla} E_{\mathbf{k}})^2 \right]}. \quad (\text{B3})$$

In deriving the first of these we have integrated by parts to evaluate

$$\begin{aligned} \frac{n}{m} &= 2 \sum_K \frac{\partial^2 \epsilon_{\mathbf{k}}}{\partial \mathbf{k} \partial \mathbf{k}} G(K) = -2 \sum_{\mathbf{k}} G^2(K) (\vec{\nabla} \epsilon_{\mathbf{k}}) \cdot \left[\vec{\nabla} \epsilon_{\mathbf{k}} + \vec{\nabla} \Sigma(K) \right] \\ &= 2 \sum_{\mathbf{k}} \frac{\Delta^2}{E_{\mathbf{k}}^2} \left[\frac{1 - 2f(E_{\mathbf{k}})}{2E_{\mathbf{k}}} + f'(E_{\mathbf{k}}) \right] \left[\varphi_{\mathbf{k}}^2 (\vec{\nabla} \epsilon_{\mathbf{k}}) \cdot (\vec{\nabla} \epsilon_{\mathbf{k}}) - \frac{1}{4} (\vec{\nabla} \epsilon_{\mathbf{k}}^2) \cdot (\vec{\nabla} \varphi_{\mathbf{k}}^2) \right] - 2 \sum_{\mathbf{k}} f'(E_{\mathbf{k}}) (\vec{\nabla} \epsilon_{\mathbf{k}}) \cdot (\vec{\nabla} \epsilon_{\mathbf{k}}). \end{aligned} \quad (\text{B4})$$

These expressions are then used to evaluate Eq. (58) in the text.

- ¹ H. Ding *et al.*, Nature (London) **382**, 51 (1996).
² A. G. Loeser *et al.*, Science **273**, 325 (1996).
³ V. J. Emery and S. A. Kivelson, Nature **374**, 434 (1995).
⁴ M. Franz and A. J. Millis, Phys. Rev. B-Condens Matter **58**, 14572 (1998).
⁵ P. A. Lee and X. G. Wen, Phys. Rev. Lett. **78**, 4111 (1997).
⁶ M. Randeria, J.-M. Duan, and L.-Y. Shieh, Phys. Rev. Lett. **62**, 981 (1989).
⁷ R. Micnas *et al.*, Phys. Rev. B **52**, 16 223 (1995).
⁸ B. Janko, J. Maly, and K. Levin, Phys. Rev. B-Condens Matter **56**, 11407 (1997).
⁹ Y. J. Uemura, Physica C **282**, 194 (1997).
¹⁰ I. Kosztin, Q. J. Chen, B. Janko, and K. Levin, Phys. Rev. B-Condens Matter **58**, R5936 (1998).
¹¹ Q. J. Chen, I. Kosztin, B. Janko, and K. Levin, Phys. Rev. Lett. **81**, 4708 (1998).
¹² J. Maly, B. Janko, and K. Levin, Phys. Rev. B-Condens Matter **59**, 1354 (1999).
¹³ O. Tchernyshyov, Phys. Rev. B-Condens Matter **56**, 3372 (1997).
¹⁴ J. Ranninger and J. M. Robin, Phys. Rev. B-Condens Matter **53**, 11961 (1996).
¹⁵ A. J. Leggett, J. Phys. (Paris) **41**, C7/19 (1980).
¹⁶ Q. J. Chen, I. Kosztin, B. Janko, and K. Levin, Phys. Rev. B-Condens Matter **59**, 7083 (1999).
¹⁷ D. M. Eagles, Phys. Rev. **186**, 456 (1969).
¹⁸ P. Nozières and S. Schmitt-Rink, J. Low Temp. Phys. **59**, 195 (1985).
¹⁹ J. J. Deisz, D. W. Hess, and J. W. Serene, Phys. Rev. Lett. **80**, 373 (1998).
²⁰ M. Randeria, <http://xxx.lanl.gov/abs/cond-mat/9710223>; M. Randeria, in *Bose-Einstein Condensation*, edited by A. Griffin, D. Snoke, and S. Stringari (Cambridge University Press, Cambridge, England, 1994).
²¹ R. Micnas, J. Ranninger, and S. Robaszkiewicz, Rev. Mod. Phys. **62**, 113 (1990).
²² N. Trivedi and M. Randeria, Phys. Rev. Lett. **75**, 312 (1995).
²³ J. M. Singer, M. H. Pedersen, and T. Schneider, Physica B **230**, 955 (1997).
²⁴ J. R. Engelbrecht, A. Nazarenko, M. Randeria, and E. Dagotto, Phys. Rev. B-Condens Matter **57**, 13406 (1998).
²⁵ J. J. Deisz, D. W. Hess and J. W. Serene, Phys. Rev. Lett. **80**, 373 (1998).
²⁶ L. P. Kadanoff and P. C. Martin, Phys. Rev. **124**, 670 (1961).
²⁷ B. R. Patton, Ph.D Thesis, Cornell University, 1971 (unpublished); Phys. Rev. Lett. **27**, 1273 (1971).
²⁸ G. Deutscher, Nature **397**, 410 (1999).
²⁹ L. Belkhir and M. Randeria, Phys. Rev. B-Condens Matter **45**, 5087 (1992).
³⁰ R. Cote and A. Griffin, Phys. Rev. B-Condens Matter **48**, 10404 (1993).
³¹ J. R. Engelbrecht, M. Randeria, and C. A. R. S. deMelo, Phys. Rev. B-Condens Matter **55**, 15153 (1997).
³² A. L. Fetter and J. D. Walecka, *Quantum theory of many-particle systems* (McGraw-Hill, San Francisc, 1971).
³³ Above T_c , the gap equation discussed below in the text, Eq. (28a), no longer holds. Instead, the LHS should be equated with a T dependent quantity, τ . Slightly above T_c , this quantity is small ($\propto (T - T_c)$), therefore, we may still use the approximation given by Eq. (22). However, the pair excitation spectrum will also acquire a T dependent gap. In consequence, we have a modified set of equations Eqs. (28) to solve for μ , Δ_{pg} , and τ above T_c . This extrapolation becomes worse as T increases.
³⁴ R. Haussmann, Z. Phys. B-Condens. Mat. **91**, 291 (1993).
³⁵ R. Haussmann, Phys. Rev. B-Condens Matter **49**, 12975 (1994).
³⁶ M. Drechsler and W. Zwerger, Ann. Physik **1**, 15 (1992).
³⁷ I. O. Kulik, O. Entin-Wohlman, and R. Orbach, J. Low Temp. Phys. **43**, 591 (1981).

³⁸ Y. Y. Zha, K. Levin, and D. Z. Liu, Phys. Rev. B-Condens Matter **51**, 6602 (1995).

³⁹ P. W. Anderson, Phys. Rev. **112**, 1900 (1958).

⁴⁰ N. N. Bogoliubov, Nuovo Cimento **7**, 794 (1958).

⁴¹ R. E. Prange, Phys. Rev. **129**, 2495 (1963).

⁴² R. A. Klemm, K. Scharnberg, D. Walker, and C. T. Rieck, Z. Phys. B-Condens. Mat. **72**, 139 (1988).

⁴³ J. R. Schrieffer, *Theory of Superconductivity*, 3rd ed. (The Benjamin/Cummings Publishing Company, Inc., Reading, Massachusetts, 1983).

⁴⁴ A. G. Aronov and V. L. Gurevich, Sov. Phys. JETP **43**, 498 (1976).

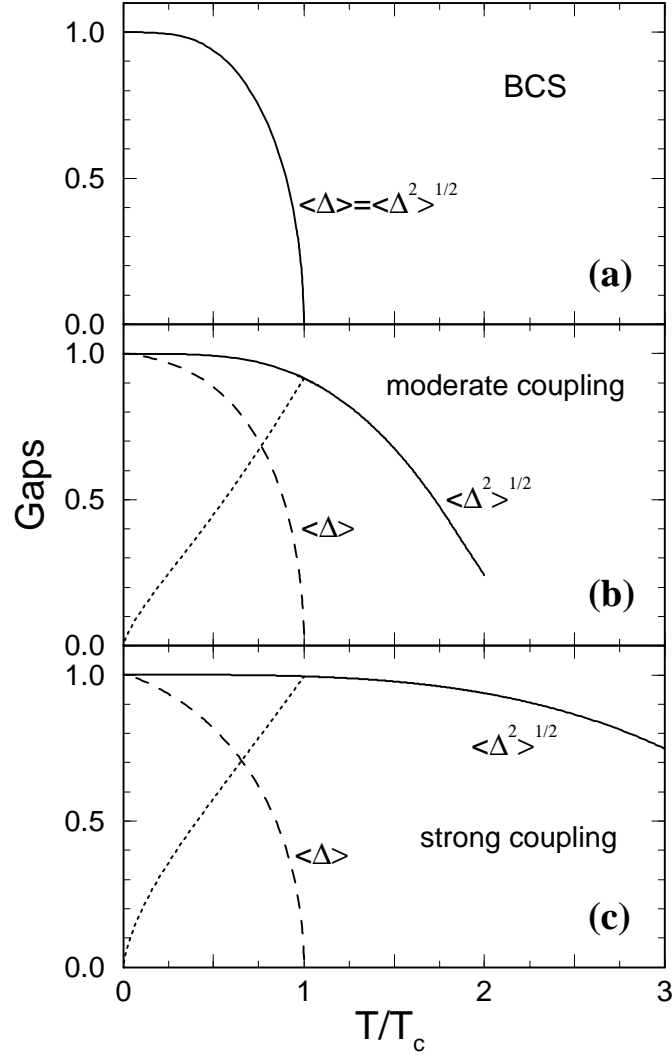


FIG. 1. Temperature dependence of the excitation gap $\langle \Delta^2 \rangle^{1/2}$ and the order parameter $\langle \Delta \rangle$ (normalized at $T = 0$) for (a) weak coupling BCS, (b) moderate coupling, and (c) strong coupling. The dotted lines represent the difference of these two energy scales, corresponding to the pseudogap parameter Δ_{pg} . A strong pseudogap develops as the coupling strength increases.

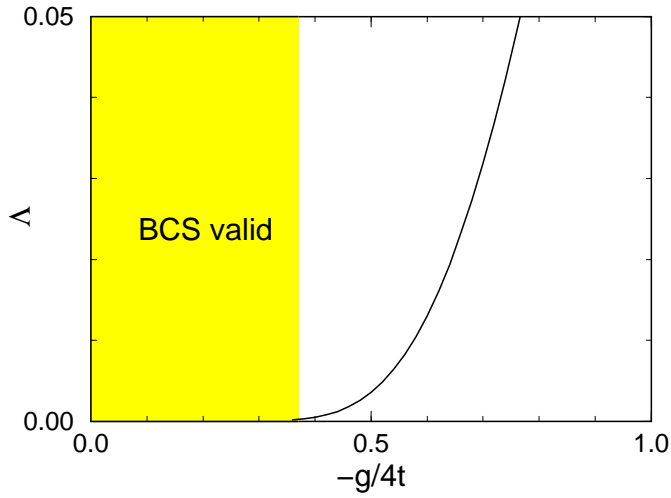


FIG. 2. Dependence of the cutoff momentum Λ , (where the pair excitation spectrum crosses into the particle-particle continuum), on the coupling strength on a quasi-2D lattice. Here $4t$ is the half bandwidth. Because of strong damping of the pair excitations, they are irrelevant at low g and BCS theory is valid in the shaded region. Outside this regime, pair excitations become important.

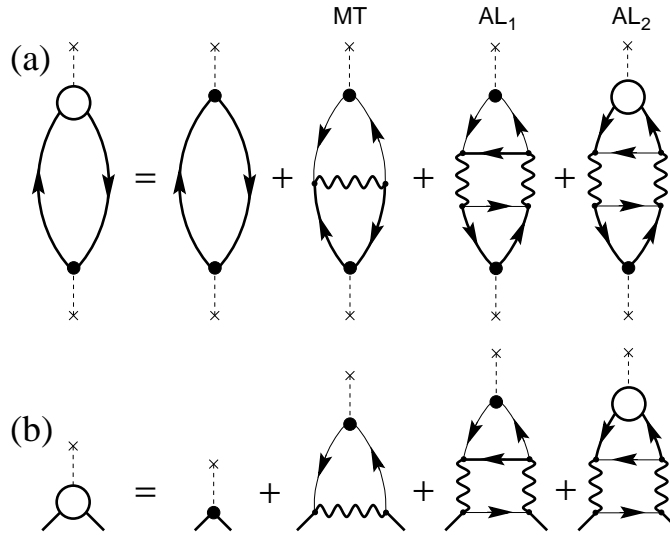


FIG. 3. Diagrammatic representation of (a) the polarization bubble, and (b) the vertex function used to compute the electrodynamic response functions. Here the wavy lines represent \mathcal{T} and it should be noted that the thin and thick lines correspond to G_o and G respectively. The total vertex correction is given by the sum of the Maki Thompson (MT) and two Aslamazov-Larkin (AL_1 and AL_2) diagrams.

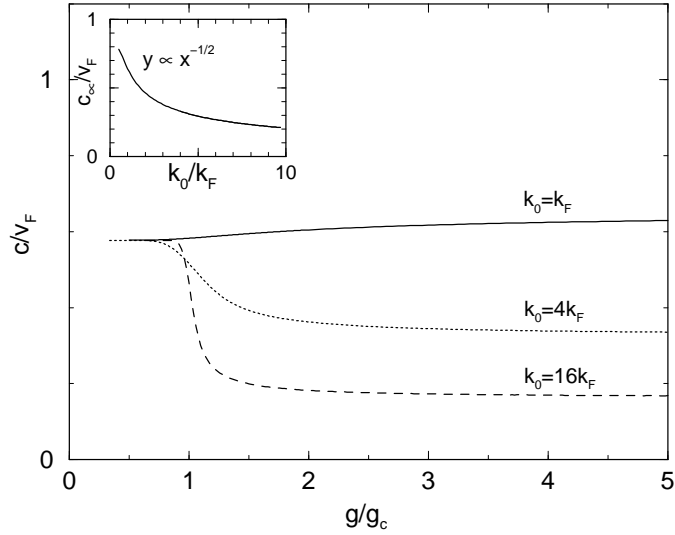


FIG. 4. AB mode velocity c/v_F as a function of the coupling strength (main figure) for various densities characterized by k_0/k_F in 3D jellium. Plotted in the inset is the large g asymptote c_∞/v_F , versus k_0/k_F , which varies as $(k_F/k_0)^{1/2}$, as expected.

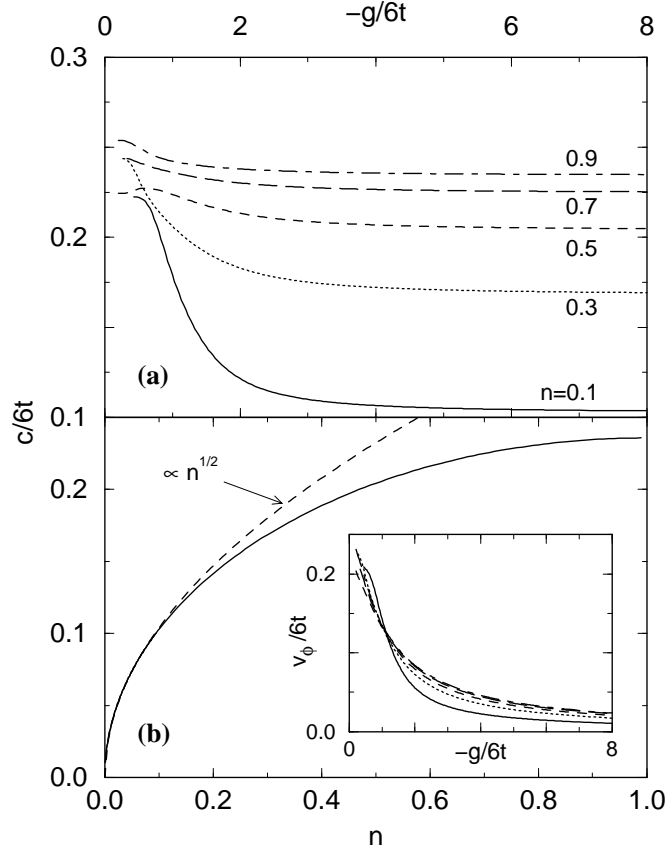


FIG. 5. (a) Normalized AB mode velocity, $c/6ta$, on a 3D lattice with an s -wave pairing interaction for various densities as a function of g , and (b) the large g limit for $c/6ta$ as a function of density n for fixed $-g/6t = 20$. (Here $6t$ is the half bandwidth). The dashed line in (b) shows a fit to the expected low density dependence $n^{1/2}$. Plotted in the inset is the velocity of the phase and density coupled collective mode $v_\phi/6ta$ with the particle-hole channel treated at the RPA level, for the same n as in (a).

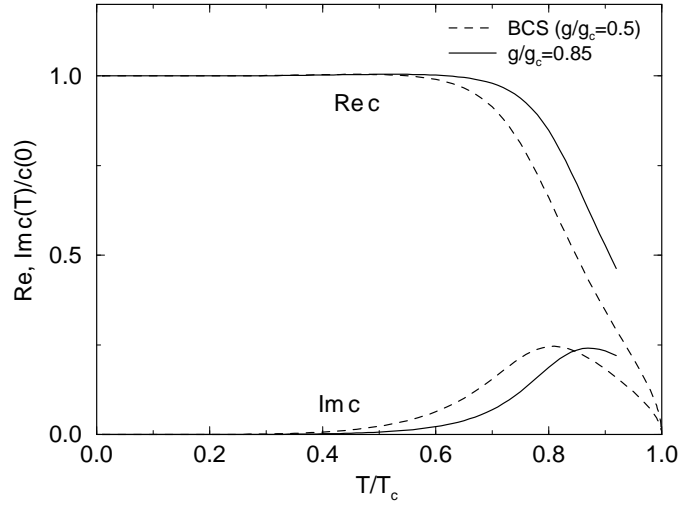


FIG. 6. Temperature dependence of the real ($\text{Re } c$) and imaginary ($\text{Im } c$) parts of the AB mode velocity for moderate coupling (solid lines) and weak coupling BCS (dashed lines) in 3D jellium with $k_0 = 4k_F$. The mode is highly damped as T_c is approached. Because of inaccuracy due to neglected T -dependent amplitude effects, the solid curves are cut off slightly below T_c .